treatment, cells were washed with PBS, and exposed to UV light (254 nm) at a fluence rate of 43 J m^{-2}/s. For genotoxin and inhibitor treatment, hydroxyurea (HU; 1 M in H_2O), aphidicolin (dissolved in Me_2SO), methyl methanesulfonate (MMS; dissolved in Me_2SO), ethyl methanesulfonate (dissolved in Me_2SO), *N*-methyl-*N*′-nitro-*N*-nitrosoguanidine (dissolved in Me_2SO), H_2O_2 (diluted in PBS), mitomycin C, bleomycin (dissolved in H_2O), or camptothecin (dissolved in Me_2SO) was added to the culture media to give a final concentration of 2 mM, 0.025 mM, 0.1–1.7 mM, 20 mM, 0.7 mM, 0.5 mM, 0.01 mM, 0.05 mg/ml, or 20 nM, respectively, and cells were exposed for 8 h unless otherwise stated.

Antibodies—A mouse monoclonal antibody against *Drosophila* RFC40 (anti-dRFC40) was used for probing human RFC2(p40). A hybridoma cell line producing anti-dRFC40 antibody was a kind gift from Dr. Gerald M. Rubin (University of California, Berkeley), and monoclonal antibody was purified as described previously (34). To test whether anti-dRFC40 antibody cross-reacts with human RFC2(p40), an HA epitope-tagged form of hRFC2(p40) was overexpressed in 293A cells by transfection, and cell lysate was recovered 24 h post-transfection and then immunoblotted with either anti-dRFC40 or anti-HA antibody. An anti-dRFC40-reactive protein band migrating at 40 kDa was clearly observed only in extracts from HA-hRFC2(p40)-transfected cells and corresponded to the species detected with an anti-HA antibody (supplemental Fig. 1). Therefore, the anti-dRFC40 antibody recognizes human RFC2(p40). To avoid confusion we refer to the anti-dRFC40 antibody as "anti-RFC2" antibody in this study.

Other commercial antibodies used in this study were: anti-HA (Y-11, Santa Cruz Biotechnology), anti-FLAG (M2, Sigma), anti-RFC1 (H-300, Santa Cruz Biotechnology), anti-RAD17 (H-3, Santa Cruz Biotechnology), anti-tubulin (B-5-1-2, Sigma), anti-histone H3 (6.6.2, Upstate; and ab1791, Abcam), and anti-PCNA (PC10, Oncogene).

Preparation of Cell Lysate and Chromatin Fraction—293A cells in a 3.5- or 6-cm dish were washed twice with ice-cold PBS and then harvested into radioimmune precipitation assay buffer (1× PBS, 1% Nonidet P-40, 0.5% sodium deoxycholate, 0.1% SDS, 1 mM phenylmethylsulfonyl fluoride, 1 mM sodium orthovanadate, and protease inhibitor (Nacalai)). The cell suspensions were incubated for 30 min on ice, and then the Nonidet P-40, 0.1% SDS-insoluble fraction and -soluble fractions were separated by centrifugation. The soluble fraction was used as the supernatant (Sup) fraction. The resultant pellet was washed with radioimmune precipitation assay buffer four times and then sonicated after adding SDS-PAGE loading buffer (7% glycerol, 22% SDS, 50 mM Tris-HCl (pH 6.8), 5% β-mercaptoethanol). The resultant solution was used as the chromatin fraction. We confirmed that there were few contaminations in each Sup and chromatin fraction using anti-tubulin and anti-histone H3 antibodies (supplemental Fig. 2).

SDS-PAGE and Western Blotting—Cell extracts were resolved by electrophoresis by 7.5 or 10% SDS-PAGE. Following transfer onto polyvinylidene difluoride or nitrocellulose filters, the blots were incubated with antibodies, and immunoblots were visualized by enhanced chemiluminescence (ECL, Amersham Biosciences; or DURA, Pierce) according to the manufacturers' instructions.

Immunoprecipitation—Cell extracts were incubated with monoclonal mouse anti-RFC2 (dRFC4(p40)) antibody for 1 h at 4 °C and then with 25 μl of protein A/G-agarose (Santa Cruz Biotechnology). After incubation for overnight at 4 °C, the beads were washed with PBS three times and boiled in Laemmli buffer for 5 min, and the bound proteins were analyzed by electrophoresis and immunoblotting.

Protein Purification—Human RFC, PCNA, and RPA were purified as described previously (29, 30). Mouse E1 was overproduced in insect cells and purified as described previously (35). Human RAD6A-RAD18 complex was overproduced in *Escherichia coli* cells and then purified by column chromatography (phosphocellulose, heparin-Sepharose, Mono Q, and gel filtration) from *E. coli* cell lysate. Protein concentrations were determined by Bio-Rad protein assay kit using bovine serum albumin as the standard. Bovine ubiquitin was purchased from Sigma.

In Vitro Ubiquitylation Assay—The reaction mixture (25 μl) contained 20 mM HEPES-NaOH (pH 7.5), 50 mM NaCl, 0.2 mg/ml bovine serum albumin, 1 mM dithiothreitol, 10 mM $MgCl_2$, 1 mM ATP, 33 fmol of singly primed single-stranded M13 mp18 DNA (30), 1.0 μg (9.1 pmol) of RPA, 86 ng (1.0 pmol as a trimer) of PCNA, 75 ng (260 fmol) of RFC, 100 ng (850 fmol) of mouse E1, 175 ng (2.4 pmol) of RAD6A-RAD18 complex, and 12.5 μg (1460 pmol) of ubiquitin. After incubation at 30 °C for 60 min, reactions were terminated with 2 μl of 300 mM EDTA.

Structural Model Building—Homology modeling of the human clamp loader-clamp complex was performed using MODELLER version 7.7 (36). The homologous structures were defined using the fold recognition server FORTE (37). The atomic coordinate of the clamp-clamp loader complex (Protein Data Bank code 1SXJ) was selected as a template for model building. Before submission to MODELLER, the sequence-structure alignment obtained from FORTE was used. Due to the lack of the template structure, the N-terminal 582 residues of human RFC1 were not modeled. The figures were prepared using MOLMOL (38). Coloring of each RFC subunit and PCNA was according to Fig. 2 in the review by Bowman *et al.* (39).

RESULTS

Specific DNA-damaging Agents Induce Modification of RFC2—To analyze the modification of each subunit of the RFC complex, a FLAG epitope-tagged form of each subunit of RFC and RLCs was expressed in human 293A cells. Transfected cells were treated with UV irradiation, γ-ray, HU, or MMS, and then cell extracts were prepared. The cell extracts were separated into Nonidet P-40-insoluble chromatin fractions and -soluble fractions (Sup). RFC and RLC subunits in each fraction were analyzed by SDS-PAGE and Western blotting (Fig. 1*A*). Following MMS treatment all of the subunits, except for CTF18 and RFC5, accumulated in the chromatin fraction, whereas no accumulation was observed following treatments with UV irradiation, γ-ray, or HU. Levels of soluble CTF18 and RFC5 decreased after MMS treatment, although we did not detect concomitant increases in the chromatin-bound levels of these

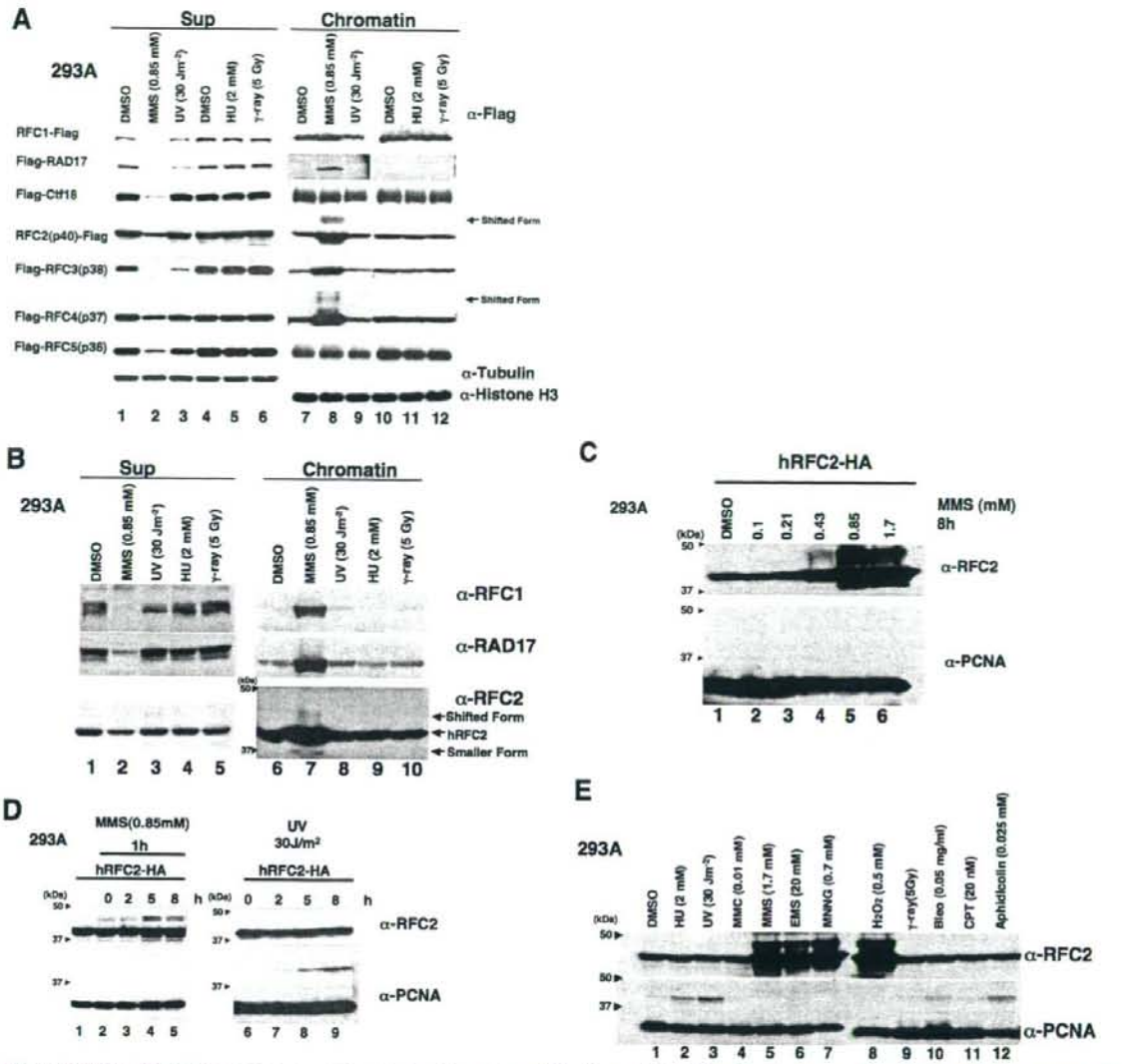

FIGURE 1. **Accumulation of RFC complex in chromatin fraction and modification of RFC2 following treatment of 293A cells with DNA-damaging agents.** *A*, 293A cells transfected with a FLAG epitope-tagged form of each subunit of RFC and RLCs were irradiated with UV light (*lanes 3* and *9*) or γ-ray (*lanes 6* and *12*) or treated with Me_2SO (*DMSO*; *lanes 1*, *4*, *7*, and *10*), MMS (*lanes 2* and *8*), or HU (*lanes 5* and *11*) for 8 h. Cell extracts recovered from transfected cells were then separated into chromatin (*lanes 7–12*) and soluble (*Sup*; *lanes 1–6*) fractions and analyzed by Western blotting with anti-FLAG. Cell extracts recovered from RFC4-transfected cells were also analyzed by Western blotting with anti-tubulin or anti-histone H3 (*lowest two blots*). *B*, 293A cells were irradiated with UV light (*lane 3*) or γ-ray (*lane 5*) or treated with Me_2SO (*lane 1*), MMS (*lane 2*), or HU (*lane 4*) for 8 h. Cell extracts recovered from transfected cells were then separated into chromatin and soluble (*Sup*) fractions and analyzed by Western blotting either with anti-RFC1, anti-RAD17, or anti-RFC2. The *arrowheads* indicate the position of molecular mass markers (kDa). *C*, 293A cells transfected with pCDNA3-RFC2-HA were treated with the indicated dose of MMS for 8 h. Chromatin fractions from the resulting cells were analyzed by immunoblotting with anti-RFC2 or anti-PCNA. The *arrowheads* indicate the position of molecular mass markers (kDa). *D*, 293A cells transfected with pCDNA3-RFC2-HA were treated with 0.85 mM MMS for 1 h (*lanes 2–5*) or UV light-irradiated at 254 nm with 30 J m^{-2} (*lanes 6–9*) and then incubated for the indicated times. Chromatin fractions were prepared and analyzed by Western blotting with anti-RFC2 and anti-PCNA. Cells treated with Me_2SO (*lane 1*) are shown as control. The *arrowheads* indicate the position of molecular mass markers (kDa). *E*, 293A cells transfected with pCDNA3-RFC2-HA were treated with various genotoxic agents. Chromatin fractions were prepared and analyzed by Western blotting with anti-RFC2 or anti-PCNA. The *arrowheads* indicate the position of molecular mass markers (kDa). *Gy*, grays; *MMC*, mitomycin C; *EMS*, ethyl methanesulfonate; *MNNG*, *N*-methyl-*N'*-nitro-*N*-nitrosoguanidine; *Bleo*, bleomycin; *CPT*, camptothecin.

subunits (Fig. 1*A*). Taken together, the results of Fig. 1*A* demonstrate that the levels and subcellular distribution of RFC and RLC subunits are regulated in response to MMS.

It was important to determine whether endogenous RFC and RLC subunits were also redistributed to chromatin in response to MMS. Therefore, we determined the effects of MMS on endogenous RFC1, RAD17, or RFC2 proteins for which good antibodies are available. As shown in Fig. 1*B*, endogenous RFC1, RAD17, and RFC2 accumulated in the chromatin fraction of MMS-treated 293A cells. Similar to

ectopically expressed tagged proteins, endogenous RFC subunits were redistributed to chromatin in response to MMS treatment.

Interestingly we observed prominent forms of ectopically expressed RFC2 and RFC4 that migrated with reduced electrophoretic mobility on SDS-PAGE gels in chromatin fractions from MMS-treated 293A cells (Fig. 1*A*, *lane 7*). Electrophoretically retarded species of endogenous RFC2 were also evident in chromatin fractions of MMS-treated 293A cells (Fig. 1*B*, *lane 7*). The electrophoretically shifted form of RFC2 was more prominent than that of RFC4 (Fig. 1*A*). Therefore we focused on RFC2 and further analyzed its MMS-induced modification.

We performed quantitative analyses to determine the amount of chromatin-bound RFC2 relative to the soluble fraction in MMS-treated cells. In 293A cells ectopically expressing HA-tagged RFC2, more than 90% of the RFC2 accumulated in the chromatin fraction following 8 h of MMS treatment, whereas in untreated cells, less than 10% of RFC2 was present in the chromatin fraction (supplemental Fig. 3). Following MMS treatment, we consistently detected two electrophoretically retarded anti-RFC2-reactive proteins in the chromatin fraction. The apparent molecular mass of electrophoretically retarded RFC2 is consistent with ubiquitylation. The two putative ubiquitylated forms of RFC2 (shown in Fig. 1) might correspond to species that are monoubiquitylated on different residues. However, we cannot exclude the possibility that modifications other than ubiquitin are also present on the shifted RFC2. Furthermore smaller anti-RFC2-reactive proteins, possibly corresponding to degradation products, were detected in soluble and chromatin fractions from both control and MMS-treated cells (Fig. 1*B* and supplemental Fig. 3).

The electrophoretically retarded forms of RFC2 were induced by MMS in a dose-dependent manner (Fig. 1*C*). At lower concentrations of MMS (0.1 or 0.213 mM), no RFC2 band shift was detectable. However, treatment with higher concentrations of MMS (0.425, 0.85, or 1.7 mM) induced prominent electrophoretically retarded forms of RFC2 on chromatin (Fig. 1*C*).

In the experiments described above, the cells were treated with MMS for 8 h. We subsequently examined the kinetics of RFC2 modification by treating 293A cells with MMS (0.85 mM) for 1 h and preparing samples for immunoblotting at 0, 2, 5, and 8 h following MMS treatment. As shown in Fig. 1*D*, the shifted forms of RFC2 were detectable by 5 h after treatment of cells with MMS (*lane 4*). Similar to results of Fig. 1*A*, the genotoxin-induced RFC2 mobility shift was specific for MMS because UV irradiation (30 J/m^2; *lanes 7–9*) did not induce RFC modification at any time point tested (although as expected, UV irradiation induced PCNA monoubiquitylation under these experimental conditions). Conversely little or no PCNA modification was detectable under the conditions used for the experiment shown in Fig. 1*D* (*lanes 2–5*), although low levels of PCNA ubiquitylation were observed when cells were treated with 0.85 mM MMS for longer times (data not shown).

The results of Fig. 1, *A* and *D*, indicated that MMS-induced RFC2 modification is not a general response to DNA damage. To gain insight into the significance of RFC2 modification, 293A cells ectopically expressing RFC2-HA were treated with a more extensive panel of DNA-damaging agents for 8 h, and proteins in resulting chromatin fractions were analyzed by immunoblotting with the anti-RFC2 antibody (Fig. 1*E*, *upper panel*). DNA-damaging agents we tested included alkylating agents (ethyl methanesulfonate and *N*-methyl-*N'*-nitro-*N*-nitrosoguanidine), an oxidizing agent (H_2O_2), a DNA cross-linking agent (mitomycin C), double strand break-inducing agents (bleomycin and ionizing radiation), and the topoisomerase I inhibitor camptothecin. Of the genotoxic agents tested, only ethyl methanesulfonate, *N*-methyl-*N'*-nitro-*N*-nitrosoguanidine, and H_2O_2 induced the shifted RFC2 band evident in MMS-treated cells (Fig. 1*E*, *upper panel*, *lanes 7–10*). Many of the agents failing to induce the RFC2 band shift nevertheless induced very robust PCNA monoubiquitylation (Fig. 1*E*, *lower panel*). Therefore, we conclude that RFC2 modification is a specific response to a subset of genotoxins.

RAD18-dependent Ubiquitylation of Human RFC2—To test whether the shifted RFC2-specific band in MMS-treated cells was due to ubiquitylation, RFC2-HA was co-expressed with FLAG-tagged ubiquitin in 293A cells. The transfected cells were treated with MMS. Endogenous and HA-tagged RFC2 proteins were immunoprecipitated with anti-RFC2 antibody from cell lysates, and the precipitated proteins were immunoblotted with either anti-RFC2 (Fig. 2*A*, *upper panel*) or anti-FLAG antibody to detect FLAG-ubiquitin-modified proteins (*lower panel*). Anti-RFC2-reactive bands migrating at the sizes expected for monoubiquitylated RFC2 (48 kDa) were observed in our anti-RFC2 immunoprecipitates (*lanes 3* and *4*, *Ub-RFC2*). In addition to the 48-kDa ubiquitin-RFC2 band, two extra, slowly migrating bands (51 and 62 kDa) were observed in the immunoprecipitates obtained from cells transfected with FLAG-tagged ubiquitin (*lane 4*, *Flag-Ub-RFC2*) that were also detectable by immunoblotting with anti-FLAG antibody (*lane 8*). From these results we conclude that the slow migrating forms of RFC2 in MMS-treated cells are ubiquitylated species.

In *S. cerevisiae* and human cells, monoubiquitylation of PCNA is dependent on the RAD18 E3 ubiquitin ligase (22, 24, 25). To determine whether ubiquitylation of RFC2 was similarly dependent on RAD18, RFC2 modification was tested in RAD18-overexpressing 293A cells (Fig. 2*B*) and *RAD18*-deficient HCT116 cells (Fig. 2*C*). As shown in Fig. 2*B*, overexpression of RAD18 induced the ubiquitylation of RFC2-HA and PCNA even in the absence of MMS treatment. Conversely MMS-induced ubiquitylated forms of RFC2 decreased considerably (by 50%) in HCT116 *RAD18*$^{-/-}$ cells compared with those in matched HCT116 *RAD18*$^{+/+}$ cells (Fig. 2*C*). These results suggest that RFC2 monoubiquitylation in MMS-treated cells is mediated at least in large part by RAD18, most probably as a complex with RAD6. Interestingly RAD18 overexpression also induced chromatin accumulation of RFC2 (Fig. 2*B*). Ubiquitylation and chromatin accumulation of RFC2 (and also RFC4) was observed in response to MMS treatment and RAD18 overexpression. Because MMS treatment induced chromatin accumulation of each RFC subunit (Fig. 1*A*), it is most likely that increased chromatin loading of the entire RFC complex occurs in response to MMS.

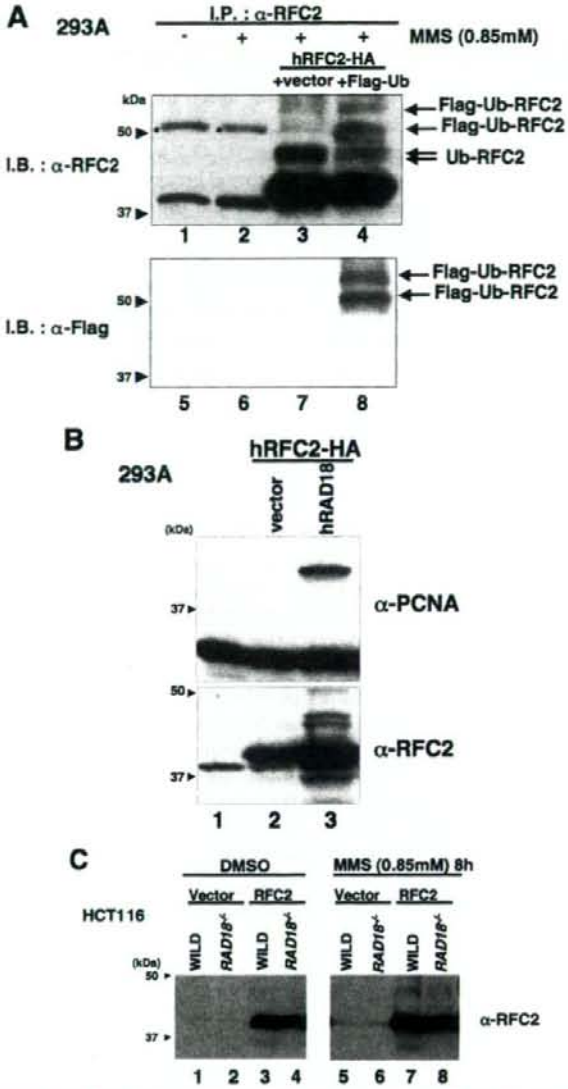

FIGURE 2. **RFC2 monoubiquitylation in response to DNA-damaging agents is RAD18-dependent.** *A*, lysates from RFC2-HA- and FLAG-ubiquitin-co-transfected 293A cells were analyzed by immunoprecipitation and Western blotting. pCDNA3·RFC2-HA was co-transfected either with pCAGGS-FLAG-Ubiquitin (*lanes 4* and *8*) or empty vector (*lanes 3* and *7*) in 293A cells. The following day, cells were treated with MMS for 8 h, and then cell extracts were recovered. Cell extracts were immunoprecipitated with anti-RFC2 antibody. The resulting immune complexes were recovered using protein A/G-agarose and detected by immunoblotting with anti-RFC2 antibody (*lanes 1–4*) or anti-FLAG antibody (*lanes 5–8*). *Asterisks* show nonspecific bands. *B*, Western blot of lysates from 293A cells overexpressing hRAD18. pCDNA3·RFC2-HA was co-transfected either with pCAGGS·hRAD18 (*lane 3*) or empty vector (*lane 2*) in 293A cells. Chromatin fractions were prepared and analyzed by Western blotting with anti-RFC2 (*lower panel*) or anti-PCNA (*upper panel*). The *arrowheads* indicate the position of molecular mass markers (kDa). *C*, Western blot of lysates from HCT116 cells (*WILD*) or *RAD18*-deficient HCT116 cells (*RAD18*$^{-/-}$). HCT116 cells transfected either with empty vector or pCAGGS·hRFC2 were treated with 0.85 mM MMS for 8 h. Chromatin fractions from the resulting cells were analyzed by immunoblotting with anti-RFC2 antibody. The *arrowheads* indicate the position of molecular mass markers (kDa). *I.P.*, immunoprecipitate; *I.B.*, immunoblot; *DMSO*, Me_2SO; *Ub*, ubiquitin.

An RFC2 Mutant Is Ubiquitylated in the Absence of DNA Damage—It has been reported that the RFC2(p40) subunit of human RFC binds the large subunit of RPA (11). In *S. cerevisiae*, a mutation in *rfc4* (yeast homolog of human RFC2(p40)) was found to display synthetic lethality with mutation in the gene encoding Rpa1 (the large subunit of *S. cerevisiae* RPA) (40). Interestingly this mutant Rfc4(p40) showed weaker physical interaction with RPA than did the wild type Rfc4(p40). This mutation, resulting in an amino acid change of aspartate to asparagine at residue 201, maps to the RFC box VIII, which is one of the conserved motifs found in all RFC subunits (16, 41). The Asp-201 residue of *S. cerevisiae* Rfc4 is conserved and found at an identical position in RFC2 from higher eukaryotes, including humans (Fig. 3*A*). We replaced Asp-228 of human RFC2 (which corresponds to *S. cerevisiae* Rfc4 Asp-201) with an asparagine residue (D228N) or an alanine (D228A). HA-tagged forms of mutant or wild-type RFC2 were expressed in 293A cells by transfection (Fig. 3*B*). The wild-type and mutant forms of RFC2-HA were expressed at similar levels; however, whereas the wild-type and D228N mutant RFC2 proteins showed no ubiquitylation of RFC2, the D228A mutant RFC2 protein underwent extensive modification without any genotoxin treatment (Fig. 3*B*, *lane 8*). The multiple shifted bands of RFC2 D228A decreased by 55% in HCT116 *RAD18*$^{-/-}$ cells compared with those in matched HCT116 *RAD18*$^{+/+}$ cells (Fig. 3*C*). Therefore, we conclude that the multiple RAD18-dependent species we observed correspond to mono- and polyubiquitylated forms of RFC2. As described in the previous sections, we observed monoubiquitylated forms of the wild-type RFC2-HA in MMS-treated cells but did not observe high levels of its polyubiquitylated forms. The results of Fig. 3*B* indicate that the RFC2 D228A mutant is extensively ubiquitylated and accumulates as multiple polyubiquitylated species (even in the absence of genotoxin treatments) when ectopically expressed. Although the difference in susceptibility to spontaneous ubiquitylation between D228A and D228N is unexpected, by analogy with the *S. cerevisiae* Rfc4 D201N mutant protein, it is most likely that Asp-228 of human RFC2 is also involved in interaction with RPA. Although we have not formally verified the reduced interaction of human RFC D228A with RPA, we infer that RAD6-RAD18-mediated RFC2 ubiquitylation is regulated by interaction with RPA (see below).

RFC2 Is Modified by the RAD6-RAD18 Complex in Vitro—We subsequently examined whether RFC2 could be modified by the RAD6-RAD18 complex *in vitro*. Recombinant RFC complex (including RFC1–5 proteins of human origin) was expressed in *E. coli* and then purified. Monoubiquitylation of RFC2 *in vitro* was investigated by mixing the RFC1–5 complex with purified recombinant RAD6A (E2 ubiquitin-conjugating enzyme)-RAD18 (E3 ubiquitin ligase) complex. As shown in Fig. 4, RFC2 was monoubiquitylated *in vitro* when incubated in the presence of purified RAD6A and RAD18 plus ubiquitin and its activating enzyme (*lane 2*) although at a much lower efficiency when compared with PCNA. It should also be noted that the *in vitro* modification of RFC2 generated only a single monoubiquitylated species, whereas at least two monoubiquitylated forms of RFC2 (corresponding to monoubiquitylation at

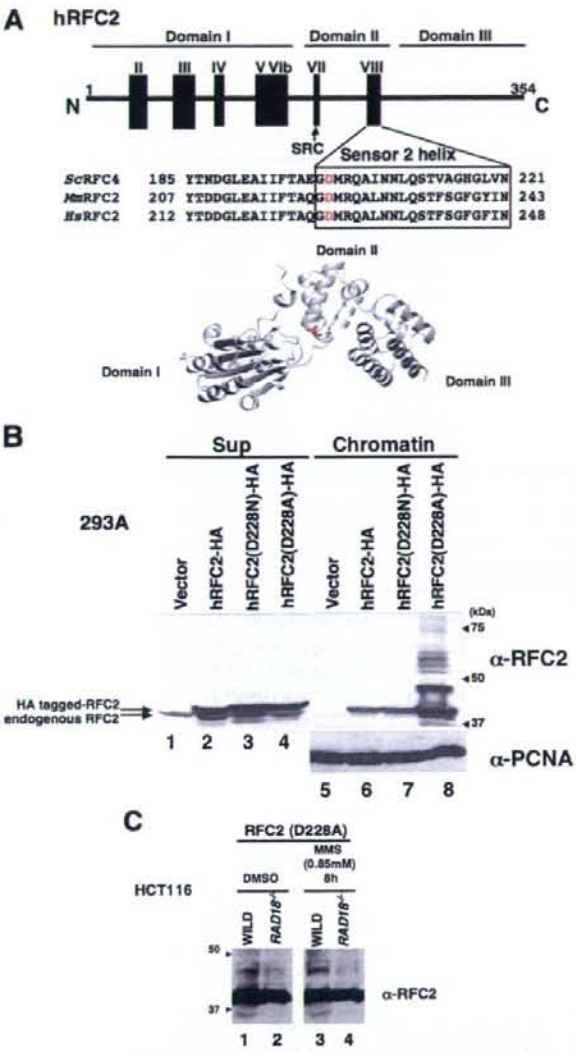

FIGURE 3. **DNA damage-independent monoubiquitylation of hRFC2 D228A.** *A*, schematic diagram and tertiary model of human (*Hs*) RFC2 showing the location of Asp-228 and the sequences of the surrounding regions. Corresponding sequences for *S. cerevisiae* (Sc) RFC2(p40) and mouse (*Mm*) RFC2 homologues are also shown. The conserved Sensor 2 helix is represented by a *box*, and the location of the conserved SRC motif is indicated by an *arrow*. Asp-228 of hRFC2, shown in *red*, corresponds to *S. cerevisiae* Asp-201, which shows synthetic lethality with mutation in Rpa-1(*rfa1*-Y29H). There are seven conserved RFC boxes *numbered* consecutively from the N terminus to C terminus. *B*, 293A cells were transfected with expression vectors encoding wild-type (*lanes 2* and *6*), D228N (*lanes 3* and *7*), or D228A (*lanes 4* and *8*) forms of hRFC2-HA. 24 h after transfection cells were harvested and separated into chromatin (*lanes 5–8*) and soluble fractions (*lanes 1–4*) and then immunoblotted with anti-RFC2 or anti-PCNA antibody. The *arrowheads* indicate the position of molecular mass markers (kDa). *C*, Western blot of lysates from HCT116 cells (*WILD*) or *RAD18*-deficient HCT116 cells (*RAD18*$^{-/-}$). HCT116 cells transfected with pCAGGS-hRFC2(Asp-228) were treated with 0.85 mM MMS for 8 h. Chromatin fractions from the resulting cells were analyzed by Western blotting with anti-RFC2 antibody. The *arrowheads* indicate the position of molecular mass markers (kDa). *DMSO*, Me_2SO.

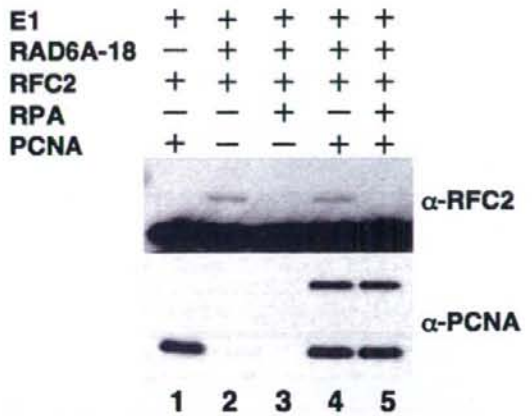

FIGURE 4. ***In vitro* monoubiquitylation of RFC2.** *In vitro* ubiquitylation was carried out by mixing RFC with mouse E1, RAD18-RAD6A complex, ubiquitin, and singly primed single stranded M13 mp18 DNA in the presence or absence of RPA or PCNA as indicated. The reaction products were analyzed by Western blotting with anti-RFC2 or anti-PCNA antibody.

different residues) resulted from MMS treatment of intact cells. The reason for the differential patterns of RAD18-mediated RFC2 monoubiquitylation observed *in vitro* and in intact cells is not yet clear but could result from the existence of additional RFC2-directed E3 ligases *in vivo*. The difference also indicates that *in vitro* assay conditions do not fully recapitulate the complexity of events involved in RPA-sensitive RFC2 ubiquitylation at stalled replication forks *in vivo*. It should be noted that our *in vitro* assay uses primed M13 single-stranded DNA, which mimics the leading strand synthesis rather than the lagging strand synthesis that requires the RFC complex more frequently. PCNA did not affect RFC2 monoubiquitylation (*lane 4*), although the modification was dependent on the presence of DNA (data not shown). Interestingly, however, the addition of RPA inhibited RAD6-RAD18-dependent monoubiquitylation completely (*lanes 3* and *5*). In parallel reactions, RPA did not affect the monoubiquitylation of PCNA (*lanes 4* and *5*). Therefore, RPA specifically inhibits RAD18-dependent monoubiquitylation of RFC2. The inhibition of RAD18-mediated RFC2 ubiquitylation by RPA *in vitro* is consistent with our finding that the RFC2 D228A mutant is more extensively modified than wild-type RFC2 in intact cells.

DISCUSSION

Protein ubiquitylation is critical for numerous cellular functions, including the DNA damage response pathway. In this study we demonstrated that RFC2 is ubiquitylated in human cells via DNA damage-independent and genotoxin-inducible mechanisms. RFC2 ubiquitylation is partially dependent on RAD18 as demonstrated by the decreased MMS-induced RFC2 ubiquitylation in *RAD18*$^{-/-}$ cells compared with matched *RAD18*$^{+/+}$ HCT116 cells (Fig. 2*C*). Conversely RFC2 undergoes genotoxin-independent monoubiquitylation in cells overexpressing RAD18. RAD18-dependent monoubiquitylation of RFC2 was also verified by *in vitro* reaction (Fig. 4). The RAD18-induced ubiquitylation of RFC2 *in vitro* and in RAD18-overexpressing cultured cells is similar to what we and others have

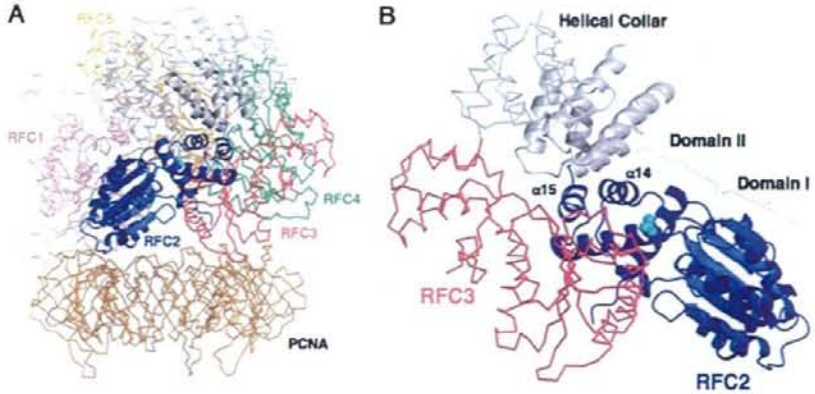

FIGURE 5. **A model for human clamp loader-clamp complex.** Ribbon (RFC2) and wire (Cα trace, RFC1, RFC3–5, and PCNA) representations of the homology model for human RFC1–5-PCNA complex are shown. The five subunits of each clamp loader complex are denoted. The colors for each of the subunits are as follows with the helical collar domains (*gray*) at the top of the figure: *pink*, RFC1; *navy*, RFC2; *red*, RFC3; *green*, RFC4; *orange*, RFC5; *gold*, PCNA. The side chain atoms of Asp-228 of RFC2 are indicated as *balls* in *cyan*. *A*, a side view of the clamp loader-clamp complex in which RFC2 is in the front. *B*, views from the DNA-interacting pore of the clamp loader subunits. Domains I and II of AAA$^+$ domain and α14 and α15 of RFC2 are indicated.

observed for PCNA, a *bona fide* RAD18 substrate. These results are further indicative of a direct E3 ligase-substrate relationship between RAD18 and RFC2.

Our *in vitro* experiments clearly show an inhibitory effect of RPA on RFC2 monoubiquitylation (Fig. 4). The involvement of RPA in regulation of RFC2 ubiquitylation *in vivo* is also suggested by our experiments with the RFC2 D228A mutant (corresponding to an *S. cerevisiae* RPA interaction-deficient Rfc4 mutant). We have shown that RFC2 D228A underwent DNA damage-independent ubiquitylation, which was reduced substantially in RAD18-deficient cells (Fig. 3*C*). Our *in vitro* assay for RAD6-RAD18-dependent RFC2 ubiquitylation did not completely recapitulate all aspects of RFC2 modification *in vivo*, and the role of RFC2 D228 in mediating RPA associations is not yet clear. However, our results strongly suggest a key regulatory role of RPA in RFC2 ubiquitylation. We propose that RAD18-dependent RFC2 ubiquitylation is repressed by RPA in undamaged cells and that derepression of RFC2 ubiquitylation occurs following MMS-induced DNA damage.

Our experiments also indicate that the RFC2 D228A mutant is subject to extensive polyubiquitylation. It is likely that polyubiquitylated RFC2 is generated by linkage of additional ubiquitin molecules to lysine residues that are first monoubiquitylated by RAD18. By analogy, following genotoxin treatments PCNA is monoubiquitylated by RAD6-RAD18 on lysine 164, and subsequently the monoubiquitylated PCNA is polyubiquitylated in a reaction mediated by MMS2-UBC13 and RAD5 (22, 23, 42, 43). It will be interesting to determine whether RAD5 or alternative E3 ligases contribute to the RAD18-initiated polyubiquitylation of RFC2. Monoubiquitylated and polyubiquitylated species of PCNA promote different damage response pathways, error-prone and error-free postreplication repair, respectively. It will be interesting to determine whether the mono- and polyubiquitylated species of RFC2 similarly serve distinct effector functions. Several studies have demonstrated that a residual level of PCNA ubiquitylation is detectable in RAD18-deficient cells. Similarly we have shown that RAD18-deficiency did not completely ablate RFC2 ubiquitylation. Clearly further work is necessary to identify the E3 ligases involved in RAD18-independent ubiquitylation of PCNA and RFC2.

To obtain insight into the question of why the RFC2 D228A mutant is susceptible to ubiquitylation without DNA damage, we constructed tertiary structure models of human RFC2 (Fig. 3*A*) and RFC complex bound to PCNA (Fig. 5) by homology modeling using the reported yeast structure (41) as the template. Each RFC subunit contains three structurally conserved domains (Domains I, II, and III). Domains I and II comprise an ATPase module of the AAA$^+$ family that is connected by a flexible linker to another helical domain (Domain III). Our structural model revealed that Asp-228 resides in the turn between helix14 and helix15 (Sensor 2 helix), which is located near the hinge region between Domains II and III (Fig. 5*C*). This implies that RFC2 Asp-228 is not exposed to the outer surface but instead is buried in the spiral structure. It is unlikely, therefore, that the Asp-228 residue directly associates with RPA as long as such a tight RFC-PCNA complex is maintained.

Whether the RFC complex remains around the primed end following PCNA loading is controversial (11, 30, 44–46). However, the RFC complex may stay associated with PCNA in a structure different from the tight complex as shown in Fig. 5*A* that allows RPA to associate with RFC2 around the Asp-228 residue. Another possibility is that the D228A mutation causes a conformational change in the RFC complex structure, possibly altering interactions with RPA and affecting susceptibility to ubiquitylation.

It is notable that RFC2 is ubiquitylated in human cells following treatment with alkylating agents but not in response to genotoxins that induce double strand breaks, bulky adducts, interstrand cross-links, or nucleotide depletion. Therefore, it appears that RFC2 monoubiquitylation is due to a specific alteration in DNA structure induced by alkylating agents or to a specific DNA repair intermediate. Identification of the DNA structure(s) responsible for RFC2 ubiquitylation may provide insight into the consequences of DNA damage due to particular genotoxins. Alkylating agents modify DNA by adding methyl or ethyl groups to a number of nucleophilic sites on the DNA bases (47). The predominant adduct in double strand DNA resulting from MMS or *N*-methyl-*N'*-nitro-*N*-nitrosoguanidine exposure is N^7-methylguanine (N^7-MeG) and N^3-methyladenine (N^3-MeA). N^3-MeA blocks replication, whereas N^7-MeG does not block replication or miscode. Another deleterious adduct is O^6-methylguanine (O^6-MeG). O^6-MeG is produced at a relatively lower level compared with N^7-MeG and N^3-MeA but is highly mutagenic and toxic because O^6-MeG-T mispairing not only results in G/C to A/T transition but also is

recognized by mismatch repair in a process that is a potent signal of apoptosis (48). However, the human kidney cell line 293A cells, which were used in this study, are mismatch repair-deficient due to epigenetic silencing of the *hMLH1* gene by promoter hypermethylation (49). Therefore, O^6-MeG is not the lesion responsible for RFC2 monoubiquitylation, and instead N^7-MeG and/or N^3-MeA are the likely candidates. Treatment of 293A cells with an oxidative agent (H_2O_2) also induced RFC2 monoubiquitylation (Fig. 1*E*). Base excision repair is the common pathway for repairing N^7-MeG, N^3-MeA, and oxidative damage (47, 50, 51). Base excision repair is initiated with removal of altered bases by DNA glycosylase. The resulting apurinic/apyrimidinic (AP) sites are nicked, and repair is completed by resynthesis and ligation. Therefore, for proficient base excision repair, a proper balance of the individual steps involved in DNA repair is important. Imbalanced base excision repair may result in deleterious intermediates, such as AP sites. Furthermore methylation or oxidation of purines destabilizes the *N*-glycosyl bond, thus rendering the base more susceptible to hydrolysis to form an AP site. Therefore, AP sites are the lesions most likely to cause RFC2 monoubiquitylation, although precisely how RPA-RFC2 interaction is affected at AP sites is unclear.

Another possible role of RFC2 ubiquitylation is as the sensing signal for damage recognition. The RFC1–5 complex (containing RFC2) has several functions. During normal DNA replication RFC1–5 acts as clamp loader for PCNA, whereas in the DNA damage response RAD17-RFC2–5 loads the 9-1-1 complex. At present we do not know whether loading of PCNA, the 9-1-1 complex, or both is affected by RAD18-dependent RFC2 modification. Experiments to further address the significance of RFC2 modification and to identify relevant effectors of modified RFC are under way.

Acknowledgments—We greatly appreciate the gift of the expression plasmids for human RPA, p11d-tRPA, from Dr. Marc S. Wold (University of Iowa College of Medicine, Iowa City, IA) and mouse E1 expression vector RLC from Dr. Hideyo Yasuda (School of Life Science, Tokyo University of Pharmacy and Life Science, Tokyo, Japan).

REFERENCES

1. Hartwell, L. H., and Weinert, T. A. (1989) *Science* **246,** 629–634
2. Carr, A. M. (2002) *DNA Repair (Amst.)* **1,** 983–994
3. Kastan, M. B., and Bartek, J. (2004) *Nature* **432,** 316–323
4. Sancar, A., Lindsey-Boltz, L. A., Unsal-Kacmaz, K., and Linn, S. (2004) *Annu. Rev. Biochem.* **73,** 39–85
5. Bochkareva, E., Korolev, S., Lees-Miller, S. P., and Bochkarev, A. (2002) *EMBO J.* **21,** 1855–1863
6. Binz, S. K., Sheehan, A. M., and Wold, M. S. (2004) *DNA Repair (Amst.)* **3,** 1015–1024
7. Kelman, Z., and O'Donnell, M. (1995) *Nucleic Acids Res.* **23,** 3613–3620
8. Wyman, C., and Botchan, M. (1995) *Curr. Biol.* **5,** 334–337
9. Fien, K., and Stillman, B. (1992) *Mol. Cell. Biol.* **12,** 155–163
10. Krishna, T. S., Kong, X. P., Gary, S., Burgers, P. M., and Kuriyan, J. (1994) *Cell* **79,** 1233–1243
11. Yuzhakov, A., Kelman, Z., Hurwitz, J., and O'Donnell, M. (1999) *EMBO J.* **18,** 6189–6199
12. Tsurimoto, T., and Stillman, B. (1991) *J. Biol. Chem.* **266,** 1961–1968
13. Maga, G., and Hubscher, U. (2003) *J. Cell Sci.* **116,** 3051–3060
14. Warbrick, E. (2000) *BioEssays* **22,** 997–1006
15. Zou, Y., Liu, Y., Wu, X., and Shell, S. M. (2006) *J. Cell. Physiol.* **208,** 267–273
16. Cullmann, G., Fien, K., Kobayashi, R., and Stillman, B. (1995) *Mol. Cell. Biol.* **15,** 4661–4671
17. Neuwald, A. F., Aravind, L., Spouge, J. L., and Koonin, E. V. (1999) *Genome Res.* **9,** 27–43
18. Kim, J., and MacNeill, S. A. (2003) *Curr. Biol.* **13,** R873–R875
19. Majka, J., and Burgers, P. M. (2004) *Prog. Nucleic Acids Res. Mol. Biol.* **78,** 227–260
20. Zernik-Kobak, M., Vasunia, K., Connelly, M., Anderson, C. W., and Dixon, K. (1997) *J. Biol. Chem.* **272,** 23896–23904
21. Wu, X., Shell, S. M., and Zou, Y. (2005) *Oncogene* **24,** 4728–4735
22. Hoege, C., Pfander, B., Moldovan, G. L., Pyrowolakis, G., and Jentsch, S. (2002) *Nature* **419,** 135–141
23. Stelter, P., and Ulrich, H. D. (2003) *Nature* **425,** 188–191
24. Kannouche, P. L., Wing, J., and Lehmann, A. R. (2004) *Mol. Cell* **14,** 491–500
25. Watanabe, K., Tateishi, S., Kawasuji, M., Tsurimoto, T., Inoue, H., and Yamaizumi, M. (2004) *EMBO J.* **23,** 3886–3896
26. Friedberg, E. C., Lehmann, A. R., and Fuchs, R. P. (2005) *Mol. Cell* **18,** 499–505
27. Bienko, M., Green, C. M., Crosetto, N., Rudolf, F., Zapart, G., Coull, B., Kannouche, P., Wider, G., Peter, M., Lehmann, A. R., Hofmann, K., and Dikic, I. (2005) *Science* **310,** 1821–1824
28. Shiomi, Y., Shinozaki, A., Nakada, D., Sugimoto, K., Usukura, J., Obuse, C., and Tsurimoto, T. (2002) *Genes Cells* **7,** 861–868
29. Fukuda, K., Morioka, H., Imajou, S., Ikeda, S., Ohtsuka, E., and Tsurimoto, T. (1995) *J. Biol. Chem.* **270,** 22527–22534
30. Masuda, Y., Suzuki, M., Piao, J., Gu, Y., Tsurimoto, T., and Kamiya, K. (2007) *Nucleic Acids Res.* **35,** 6904–6916
31. Henricksen, L. A., Umbricht, C. B., and Wold, M. S. (1994) *J. Biol. Chem.* **269,** 11121–11132
32. Honda, R., Tanaka, H., and Yasuda, H. (1997) *FEBS Lett.* **420,** 25–27
33. Imai, N., Kaneda, S., Nagai, Y., Seno, T., Ayusawa, D., Hanaoka, F., and Yamao, F. (1992) *Gene (Amst.)* **118,** 279–282
34. Harrison, S. D., Solomon, N., and Rubin, G. M. (1995) *Genetics* **139,** 1701–1709
35. Haas, A. L., and Bright, P. M. (1988) *J. Biol. Chem.* **263,** 13258–13267
36. Fiser, A., and Sali, A. (2003) *Methods Enzymol.* **374,** 461–491
37. Tomii, K., and Akiyama, Y. (2004) *Bioinformatics (Oxf.)* **20,** 594–595
38. Koradi, R., Billeter, M., and Wuthrich, K. (1996) *J. Mol. Graph.* **14,** 29–32
39. Bowman, G. D., Goedken, E. R., Kazmirski, S. L., O'Donnell, M., and Kuriyan, J. (2005) *FEBS Lett.* **579,** 863–867
40. Kim, H. S., and Brill, S. J. (2001) *Mol. Cell. Biol.* **21,** 3725–3737
41. Bowman, G. D., O'Donnell, M., and Kuriyan, J. (2004) *Nature* **429,** 724–730
42. Motegi, A., Sood, R., Moinova, H., Markowitz, S. D., Liu, P. P., and Myung, K. (2006) *J. Cell Biol.* **175,** 703–708
43. Unk, I., Hajdu, I., Fatyol, K., Szakal, B., Blastyak, A., Bermudez, V., Hurwitz, J., Prakash, L., Prakash, S., and Haracska, L. (2006) *Proc. Natl. Acad. Sci. U. S. A.* **103,** 18107–18112
44. Gomes, X. V., and Burgers, P. M. (2001) *J. Biol. Chem.* **276,** 34768–34775
45. Podust, V. N., Tiwari, N., Stephan, S., and Fanning, E. (1998) *J. Biol. Chem.* **273,** 31992–31999
46. Moldovan, G. L., Pfander, B., and Jentsch, S. (2007) *Cell* **129,** 665–679
47. Wyatt, M. D., and Pittman, D. L. (2006) *Chem. Res. Toxicol.* **19,** 1580–1594
48. Stojic, L., Brun, R., and Jiricny, J. (2004) *DNA Repair (Amst.)* **3,** 1091–1101
49. Trojan, J., Zeuzem, S., Randolph, A., Hemmerle, C., Brieger, A., Raedle, J., Plotz, G., Jiricny, J., and Marra, G. (2002) *Gastroenterology* **122,** 211–219
50. Hoeijmakers, J. H. (2001) *Nature* **411,** 366–374
51. Krokan, H. E., Nilsen, H., Skorpen, F., Otterlei, M., and Slupphaug, G. (2000) *FEBS Lett.* **476,** 73–77

16. ヒト REV1 による損傷乗り越え DNA 合成の生化学的解析

朴　金蓮・増田　雄司・神谷　研二

Ⅰ. 緒　　言

電離放射線は，DNA のさまざまな部位に作用し，酸化的 DNA 損傷を引き起こす。DNA 損傷の多くは，DNA 合成の際に正常な塩基対合を妨げることにより DNA 複製を強く阻害する。DNA 複製の阻害は細胞にとって致死的であるため，これを回避するための細胞応答機構が重要な役割をもつ。損傷乗り越え DNA 合成（translesion synthesis, TLS）機構は，損傷特異的な DNA ポリメラーゼが，損傷部位での DNA 合成反応を行い，DNA 複製を回復する機能を持つ。TLS は DNA 損傷に対する細胞応答の一つであり，DNA 修復機構とともに染色体の恒常性維持に必要不可欠な生物機能である。

酵母で同定された *REV* 遺伝子群は TLS に関与し，放射線による突然変異の誘発に重要な役割を担っている[1]。われわれはこれまでに，REV1 タンパク質は，*umuC/dinB/XPV* ファミリーの遺伝子がコードする Y ファミリー損傷乗り越え型 DNA ポリメラーゼに属し，酸化的 DNA 損傷の TLS を効率よく行うことを明らかにした[2)-5)]。

色素性乾皮症の原因遺伝子である *XPV* がコードする pol η は同じ Y ファミリーに属し，紫外線による DNA 損傷の一つであるチミンダイマーに対して正しく dAMP を取り込み，損傷部位を正しく乗り越える[6]。一方，REV1 には DNA ポリメラーゼ活性はなく，酸化的 DNA 損傷に対して唯一 dCMP を取り込む[1]。この活性は進化的にとてもよく保存されていることから，損傷部位に対する dCMP の取り込みが，生体防御において重要な活性であることが示唆されているが，その生物学的意義は今のところ不明である。

当研究室では，これまでに，ヒト REV1 タンパク質による損傷乗り越え DNA 合成の分子機構を明らかにするため，組み換え REV1 タンパク質を精製し，その生化学的解析を行ってきた。REV1 は鋳型 G に対して，dCMP，dGMP，dTMP を挿入し，dCMP を取り込む反応が最も効率高いことが明らかとなった。また，鋳型 A，T，C に対して dCMP を挿入し，電離放射線によって生じる DNA 損傷の一つ，脱塩基部位（AP site）に対して，dCMP を効率よく取り込むことが分かった。今回われわれは上述の鋳型以外に，酸化的 DNA 損傷により生ずる U（ウラシル），8-オキソグアニン（8-oxoguanine），またアルキル化剤により生じる O^6-メチルグアニン（O^6-methylguanine）など損傷部位を持つ鋳型を使って，REV1 の損傷乗り越え活性を調べた。その結果，REV1 はさまざまな，損傷部位に dCMP を効率的に取り込むことで，DNA 損傷乗り越え活性を持つことが分かった。

Ⅱ. 材料と方法

組み換え REV1 タンパク質は，ヒスタグ融合タンパク質として大腸菌で過剰生産させた後，ニッケル親和性クロマトグラフィー，ゲル濾過クロマトグラフィーにより精製した。精製したタンパク質の dNMP 転移活性は，プライマー伸長反応として検出した[2)-5)]。

Ⅲ. 結　　果

REV1 の損傷鋳型塩基に対する基質特異性を測定するために，図 1 に示した U（ウラシル），脱塩基部位（AP site），O^6-メチルグアニン（O^6-methylguanine），8-オキソグアニン（8-oxoguanine）など鋳型 DNA を用いて dGTP，dATP，dTTP，dCTP それぞれまたは，4 種類の dNTP の存在下でプライマー伸長反応を行った。その結果，REV1 の鋳型 G に対して dCMP を選択的に取り込むのに対して，U（ウラシル），AP（脱塩基部位），G-6me（O^6-メチルグアニン），G-8oxo（8-オキソグアニン）に対しても dCMP を選択的に取り込むことが分かった。また，G-8oxo（8-オキソグアニン）に対しては，dGMP，dTTP も

JinLian Piao, Yuji Masuda, Kenji Kamiya: Biochemical analysis of deoxytidyl transferase axtivity of human REV1. Department of Experimental Oncology, Research Institute for Radiation Biology and Medicine, Hiroshima University.
広島大学原爆放射線医科学研究所ゲノム障害制御研究部門分子発がん制御研究分野

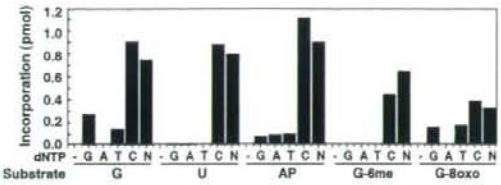

図 1　REV1 プライマー伸長反応産物の解析

図の横軸は，デオキシヌクレオチドと基質（substrate）を示している。5' 末端を ^{32}P で標識した 13-mer のプライマーと 30-mer の鋳型 DNA をアニーリングさせた。基質は G と損傷鋳型 DNA はそれぞれプライマー末端のすぐ下流の鋳型塩基 G，U（ウラシル），AP（脱塩基部位），G-6me（O^6-メチルグアニン），G-8oxo（8-オキソグアニン）に対するデオキシヌクレオチドの取り込みを測定することができる。上述の鋳型 DNA と REV1 を図に示した 4 種類の dNTP（G, A, T, C）のそれぞれ，またはそれらの混合物（N）の存在下でプライマー伸長反応を行い，反応産物を変性アクリルアミドゲル電気泳動し，オートラジオグラフィーにより解析した。(-) は dNTP なしのコントロール。図の縦軸は，デオキシヌクレオチドの取り込み効率を示している。

取り込むことが検出された。これらの結果から，ヒト REV1 は，損傷 DNA に対して dCMP を選択的に取り込むことで損傷を乗り越えることが実験的に証明された。

IV. 考　　察

本研究でわれわれは，REV1 はさまざまな損傷部位に dCMP を効率的に取り込むことで，DNA 損傷を乗り越え活性を持つことが分かった。今後は，変異型 REV1 の損傷を乗り越え基質特異性の詳細な生化学解析を行い，dCMP transferase 活性の生物学的意義を明らかにしたいと考えている。

V. 結　　語

REV1 の損傷 DNA に対して dCMP を選択的に取り込むことで損傷を乗り越えることが実験的に証明された。

文　　献

1) Nelson JR, Lawrence CW, et al: Deoxycytidyl transferase activity of yeast REV1 protein, Nature: 382: 729–731, 1996.
Masutani C, Kusumoto, R et al: The XPV (xeroderma pigmentosum variat) gene encodes human DNA polymerase h, Nature: 399: 700–704, 1999.

2) Masuda Y, Takahashi M, et al: Deoxycytidyl transferase activity of the human REV1 protein is closely associated with the conserved polymerase domain, J Biol Chem: 276: 15051–15058, 2001.

3) Masuda Y, Takahashi M, et al: Mechanisms of dCMP Transferase Reaction Catalyzed by Mouse Rev1 protein, J Biol Chem: 277: 3040–3046, 2002.

4) Masuda Y, Kamiya K: Biochemical properties of the human REV1 protein, FEBS Letters 520: 88–92, 2002.

5) Masuda Y, Ohmae M, et al: Structure and enzymatic properties of a stable complex of the human REV1 and REV7 proteins, J Boil Chem 278: 12356–12360, 2003.

6) Masutani C, Kusumoto R, et al: The XPV (xeroderma pigmentosum variant) gene encodes human DNA polymerase η, Nature: 399: 700–704, 1999.

RADIATION RESEARCH 170, 216–223 (2008)
0033-7587/08 $15.00

Absence of *Ku70* Gene Obliterates X-Ray-Induced *lacZ* Mutagenesis of Small Deletions in Mouse Tissues

Yoshihiko Uehara,[a] Hironobu Ikehata,[a] Jun-ichro Komura,[a] Ari Ito,[a] Masaki Ogata,[a] Tsunetoshi Itoh,[a] Ryoichi Hirayama,[b] Yoshiya Furusawa,[b] Koichi Ando,[b] Tatjana Paunesku,[c] Gayle E. Woloschak,[c] Kenshi Komatsu,[d] Shinya Matsuura,[e] Tsuyoshi Ikura,[a] Kenji Kamiya[e] and Tetsuya Ono[a,1]

[a] *Department of Cell Biology, Graduate School of Medicine, Tohoku University, 2-1 Seiryo-machi, Aoba-ku, Sendai 980-8575, Japan;* [b] *Heavy-Ion Radiobiology Research Group, National Institute of Radiological Sciences, Anagawa 4-9-1, Inage-ku, Chiba 263-8555, Japan;* [c] *Department of Radiology, Feinberg School of Medicine, Northwestern University, Chicago, IL 60611;* [d] *Department of Genome Repair Dynamics, Radiation Biology Center, Kyoto University, Yoshida-konoe, Sakyo-ku, Kyoto 606-8501, Japan; and* [e] *Research Institute for Radiation Biology and Medicine, Hiroshima University, Kasumi-ku, Hiroshima 734-8553, Japan*

Uehara, Y., Ikehata, H., Komura, J-I., Ito, A., Ogata, M., Itoh, T., Hirayama, R., Furusawa, Y., Ando, K., Paunesku, T., Woloschak, G. E., Komatsu, K., Matsuura, S., Ikura, T., Kamiya, K. and Ono, T. Absence of *Ku70* Gene Obliterates X-Ray-Induced *lacZ* Mutagenesis of Small Deletions in Mouse Tissues. *Radiat. Res.* 170, 216–223 (2008).

With the goal of understanding the role of non-homologous end-joining repair in the maintenance of genetic information at the tissue level, we studied mutations induced by radiation and subsequent repair of DNA double-strand breaks in *Ku70* gene-deficient *lacZ* transgenic mice. The local mutation frequencies and types of mutations were analyzed on a *lacZ* gene that had been chromosomally integrated, which allowed us to monitor DNA sequence alterations within this 3.1-kbp region. The mutagenic process leading to the development of the most frequently observed small deletions in wild-type mice after exposure to 20 Gy of X rays was suppressed in *Ku70*$^{-/-}$ mice in the three tissues examined: spleen, liver and brain. Examination of DNA break rejoining and the phosphorylation of histone H2AX in *Ku70*-deficient and -proficient mice revealed that *Ku70* deficiency decreased the frequency of DNA rejoining, suggesting that DNA rejoining is one of the causes of radiation-induced deletion mutations. Limited but statistically significant DNA rejoining was found in the liver and brain of *Ku70*-deficient mice 3.5 days after irradiation, showing the presence of a DNA double-strand break repair system other than non-homologous end joining. These data indicate a predominant role of non-homologous end joining in the production of radiation-induced mutations *in vivo*. © 2008 by Radiation Research Society

INTRODUCTION

DNA double-strand breaks cause serious problems for cells because their presence leads to losses of small and large DNA fragments. Two kinds of DNA repair systems are known to work to rejoin these breaks: non-homologous end joining (NHEJ) and homologous recombination repair (HRR). In many higher organisms, NHEJ has been shown to play a major role in genome maintenance. NHEJ occurs through the collaboration of several proteins, including Ku70, Ku80, DNA-PKcs, ligase IV and Cernunnos-XLF (*1–6*). Inactivation of the NHEJ system by knocking out one of the key genes in this repair pathway results in severe health problems including immunodeficiency, developmental abnormalities, early cancer development, and premature aging. Among these, cancer and premature aging are assumed to be induced at least in part by genomic instability caused by the lack of repair of spontaneously occurring DNA double-strand breaks (*1–4, 7, 8*). However, this assumption is not clearly established. Genomic alterations induced by DNA double-strand breaks are grouped into two categories: (1) large-scale changes such as chromosomal fragmentation, rearrangement of large DNA fragments, and telomere defects; (2) alteration of DNA at the gene sequence level, resulting in gene mutations. Studies on chromosomal structures in untreated NHEJ-deficient cultured cells showed elevated levels of fragmented and translocated chromosomes (*9–11*). Untreated NHEJ-deficient mice with an inactivated *Ku80* gene, on the other hand, had a reduced level of spontaneous large-scale DNA rearrangements compared to wild-type mice as judged by a chromosomally integrated *lacZ* gene enclosed in plasmid DNA (*12*). The discrepancy could be explained by elimination of cells containing chromosomal rearrangements *in vivo* by apoptosis, although little evidence is available to support this. Irradiation of cultured cells induces chromosomal abnormalities, which become even more frequent in NHEJ-deficient cells (*13*). This finding was supported by biochemical analyses of DNA rejoining using pulsed-field gel electrophoresis combined with Southern blot analysis (*14*). NHEJ deficiency resulted in the suppression of rejoining of 50% of the

[1] Address for correspondence: Department of Cell Biology, Graduate School of Medicine, Tohoku University, 2-1 Seiryo-machi, Aoba-ku, Sendai 980-8575, Japan; e-mail: tono@mail.tains.tohoku.ac.jp.

radiation-induced DNA double-strand breaks—a finding that is in agreement with elevated chromosomal fragment formation in irradiated NHEJ-deficient cells (*13*). Interestingly, the remaining 50% of the breaks were rejoined correctly in both wild-type and NHEJ-deficient cells, indicating the presence of an error-free repair system working independently from NHEJ. The method, however, identifies DNA of Mbp sizes and does not detect DNA alterations of less than a few hundred kbp. Thus the correct rejoining in the context of these published studies does not reflect the degree of DNA sequence maintenance at the nucleotide level such as base substitutions and short-fragment DNA deletions and insertions. More detailed studies were done with mutation analysis. However, the mutation studies performed on the cultured cells for the effect of NHEJ deficiency were complicated. The spontaneous mutation levels of both the *TK* and *HPRT* genes were not affected by DNA-PKcs deficiency, and radiation-induced mutation was suppressed at the *TK* locus but not at the *HPRT* locus (*15*). Ku-deficient Chinese hamster cells were shown to be sensitive to mutation induction at the *HPRT* locus using bleomycin, a drug that induces DNA double-strand breaks (*16*). *In vivo* studies of the role of NHEJ for radiation-induced mutation of single genes have not been performed previously.

Previously, we studied the molecular nature of mutations induced by radiation in mouse tissues using a chromosomally integrated *lacZ* gene enclosed in lambda DNA as a marker, and we found that the predominant type of mutation was deletion of one to a few hundred base pairs (*17*). Similar results were observed subsequently in a gpt delta transgenic mouse (*18*). This type of mutation is shown to be produced through errors associated with NHEJ repair of DNA double-strand breaks that were created either in the process of DNA rearrangement of antigen-receptor genes (*19*) or by restriction enzyme-induced double-strand breaks (*20–22*). Therefore, we postulated that NHEJ could be responsible for the major type of mutation found in tissues as a consequence of radiation exposure. We analyzed mutant frequencies and the molecular nature of the mutants as well as rejoining of DNA breaks in *Ku70*-knockout *lacZ* transgenic mice. Since the genome maintenance system in each tissue is unique and DNA repair and the mutational burden vary among different tissues (*23–27*), we examined three tissues with different cell renewal properties: spleen, liver and brain.

MATERIALS AND METHODS

Mice

Muta™ mice, which harbor the *lacZ*-containing lambda phage genome as a transgene (*28*), were purchased from Covance Research Products, Denver, PA. The genetic background of the mice was a mixture of BALB/c and DBA/2 (*28*). The Muta™ mice were mated with $Ku70^{+/-}$ mice (*29*). F_1 mice of the $Ku70^{+/-}$, $lacZ^+$ genotype were selected and mated again to obtain $Ku70^{-/-}$, $lacZ^+$; $Ku70^{+/-}$, $lacZ^+$; and $Ku70^{+/+}$, $lacZ^+$ mice. The genotype of *Ku70* was determined by PCR as described previously (*29*). The PCR primers for *lacZ* were 5′-(-84)CACCCCAGGCTTTACACTTT (sense primer) and 5′-(2525)ATCAGCACCGCATCAGCAAG (antisense primer). The PCR conditions were 94°C for 4 min followed by 28 cycles of 94°C for 30 s, 55°C for 1 min and 72°C for 1 min and a final incubation at 72°C for 4 min (*30*).

Irradiation

Two-month-old mice were placed in a plastic box in which they could move freely and were irradiated with 20 or 50 Gy of X rays (200 kVp, 10 mA, filtered with 1 mm aluminum and 0.5 mm copper, 0.72 Gy/min, Shimadzu HF320, Kyoto, Japan). For the analysis of DNA fragmentation, mice were irradiated at a higher dose rate to minimize DNA rejoining during irradiation (220 kVp, 17 mA, filtered with 0.5 mm aluminum and 0.3 mm copper, 5.83 Gy/min). The tissues were harvested immediately (2 to 3 min), 1 h or 3.5 days after irradiation. The animal experiments were conducted according to the Guidelines for Animal Welfare and Experimentation at Tohoku University.

Mutation Assay

Mutant frequencies were determined at 3.5 days after irradiation. Genomic DNA was isolated from tissues by phenol extraction and mixed with lambda phage packaging extract (Transpack® Packaging Extract, Stratagene, La Jolla, CA). The number of phages retrieved containing the *lacZ* gene was estimated by the number of plaques that developed on *E. coli* strain C of galE⁻. The number of phages containing a mutated *lacZ* gene was counted as plaques observed in the presence of phenyl-β-D-galactose. Two or three $Ku70^{+/+}$ and $Ku70^{+/-}$ mice and three or four $Ku70^{-/-}$ mice were examined.

Sequencing of the mutant *lacZ* gene was done by a DNA sequencer (ABI PRISM™ 3100, Applied Biosystems, Foster City, CA), and the sequences obtained were compared to the nucleotide sequence of the wild-type *lacZ* gene. For the analysis of the mutation spectrum, two or more mutants showing identical characteristics to the other mutant found in the same DNA preparation were eliminated from counting to avoid a possible effect of replication of mutation. The details of this procedure were described previously (*24, 30*).

SFGE Analysis of DNA Breaks

To monitor DNA breaks and rejoining, static-field gel electrophoresis (SFGE) was used (*31*). A part of the spleen or liver or a longitudinal half of a brain was minced with a pair of scissors, dissolved in phosphate-buffered saline, pipetted about 10 times to disassociate cells, strained through a 40-μm mesh strainer (BD Falcon, Bedford, MA), and rinsed twice by centrifugation. The spleen cell density was adjusted to 2.5×10^7 cells/ml. The liver and brain cell suspensions were adjusted to $OD_{600} = 12$ using a spectrophotometer, because the cells were difficult to count. The cell suspension (15 μl) was embedded in 55 μl of 1.3% agarose and lysed with lysis buffer and proteinase K at 50°C, 24 h (CHEF Genomic DNA Plug Kits, Bio-Rad Laboratories, Hercules, CA). The DNA was electrophoresed for 36 h at 0.6 V/cm. The DNA remaining in the well and the DNA released into the gel were quantified after staining with ethidium bromide. The details of this procedure were described previously (*31*). The fraction of DNA released from the wells was used as a measure of DNA breaks.

Western Blot Analysis of γ-H2AX

Approximately 0.1 g of spleen or 0.3 g of liver was minced with a pair of scissors and homogenized in a glass homogenizer in lysis buffer containing 0.5% Triton X-100. For brain, a longitudinal half of a whole organ was used. The homogenized samples were centrifuged at 800*g* for 2 min, and the precipitated nuclei were rinsed again with lysis buffer. The nuclei were lysed with 1% of SDS, and the DNA was fragmented by sonication. After the insoluble material was pelleted, nuclear proteins were separated by 15% SDS-polyacrylamide gel electrophoresis, trans-

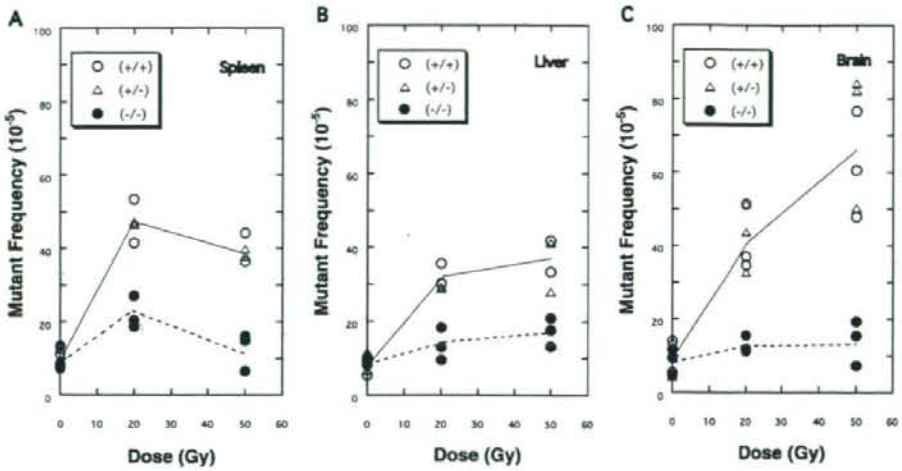

FIG. 1. Effects of *Ku70* genotype on radiation-induced *lacZ* mutations in the spleen (panel A), liver (panel B) and brain (panel C) of Muta™ mouse. Mutant frequencies after whole-body exposure to 0, 20 and 50 Gy radiation were examined in $Ku70^{+/+}$, $^{+/-}$ and $^{-/-}$ *lacZ* transgenic mice. No difference was observed between $Ku70^{+/+}$ and $^{+/-}$ mice.

ferred to nitrocellulose membranes, and analyzed for H2AX and phosphorylated H2AX (γ-H2AX) using antibodies specific for each protein; anti-H2AX Ab was made using the C terminal peptide of human H2AX as an antigen; a monoclonal Ab for γ-H2AX [Phospho-Histone H2AX (Ser139)] was purchased from Cell Signaling Technology Inc., Danvers, MA). The procedures have been described elsewhere (*32*). Non-phosphorylated and phosphorylated H2AX were compared by Western blots as an indication of the presence of DNA breaks in cells (*33*).

RESULTS

Radiation-Induced Mutations

The mutant frequencies in spleen, liver and brain after exposure to 0, 20 or 50 Gy X rays are shown in Fig. 1. $Ku70^{+/+}$ and $^{+/-}$ mice showed increased mutation frequencies after irradiation, whereas $Ku70^{-/-}$ mice showed reduced mutation levels in all three tissues compared to *Ku70*-proficient mice. $Ku70^{+/+}$ and $^{+/-}$ mice had no appreciable differences. The spontaneous levels of mutations were similar for all three genotypes. The number of mutations induced by 20 Gy were calculated by subtracting the average mutant frequency of nonirradiated mice from that of irradiated mice. The numbers of induced mutations in *Ku70*-proficient and -deficient mice were compared to determine the percentages of mutations produced through a *Ku70*-dependent NHEJ process; they were 67, 82 and 86% in spleen, liver and brain, respectively.

To understand the molecular mechanisms underlying these differences, we sequenced the *lacZ* DNA of the mutant clones. The frequencies of the different types of mutations are shown in Fig. 2. In $Ku70^{+/+}$ and $^{+/-}$ mice, the predominant type of mutation induced by radiation was a deletion, whereas this type of mutation was much less frequent in $Ku70^{-/-}$ mice. The results were similar in all three tissues we examined. This indicates that the predominant type of mutation induced by radiation at the gene sequence level, a deletion, is produced through a *Ku70*-dependent NHEJ process.

Recently, Honma *et al.* reported that the predominant mutations produced at double-strand break sites made by restriction enzyme I-*Sce*I were 1- to 50-bp-long deletions (*22*). Hence we classified the deletion mutations we found into two groups: 1–50 bp and more than 50 bp (Table 1). All of the spontaneous mutations were in the former group, whereas radiation induced deletion mutations of both sizes. In *Ku70*-proficient irradiated mice, 1–50 bp was predominant, but this was not the case in *Ku70*-deficient irradiated mice (Table 1). In other words, *Ku70* deficiency results in the suppression of small deletions of 1 to 50 bp rather than the larger deletions.

Details about the infrequent mutations classified as multiple and complex mutations in Fig. 2 are presented in Table 2. These types of mutations are observed only in irradiated mice, with the exception of one found in the unirradiated spleen of the $Ku70^{-/-}$ mouse. The complex-type mutations can be explained by the deletion of a small number of nucleotides with a simultaneous insertion of a few nucleotides at the same site. This type of mutation was reported previously in wild-type Muta™ mice (*17*) and gpt delta transgenic mice (*18*) after irradiation. The multiple mutations we encountered can be grouped into two categories: (1) two or three changes within 14 nucleotides and (2) two alterations observed separately with a distance of 558 bp or more. Interestingly, the latter class of mutation was found only in irradiated $Ku70^{-/-}$ mice (four cases) and not in unirradiated mice or irradiated *Ku70*-proficient mice. We found 188 independent mutations in irradiated *Ku70*-pro-

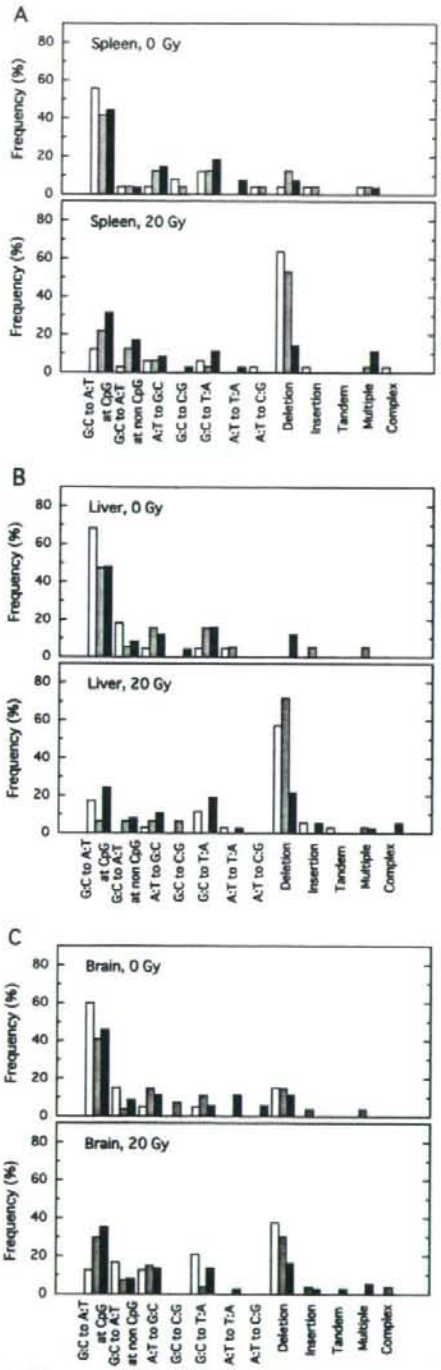

FIG. 2. Mutation spectra in nonirradiated and 20 Gy-irradiated *Ku70*$^{+/+}$, $^{+/-}$ and $^{-/-}$ *lacZ* transgenic mice 3.5 days postirradiation. The frequencies of different types of mutations revealed by sequencing of mutant clones are shown. Open, gray and black columns represent wild-type mice, *Ku70*$^{+/-}$ mice and *Ku70*$^{-/-}$ mice, respectively. Deletion-type mutations were induced by irradiation of *Ku70*$^{+/+}$ and $^{+/-}$ mice, but they were not prominent in $^{-/-}$ mice.

ficient mice and 109 in irradiated *Ku70*-deficient mice. Fisher's exact probability test showed that the number of multiple mutations appearing separately at a distance of more than 558 bp was significantly higher in *Ku70*$^{-/-}$ mice (4/109) than in *Ku70*-proficient mice (0/188, $P = 0.0175$).

DNA Breaks and Rejoining

The suppression of radiation-induced mutation in *Ku70*-deficient mice could be explained by lack of rejoining of DNA double-strand breaks, which would not be detected as mutations, or by repair through homologous recombination, which is known to be error-free. To obtain more information, we analyzed DNA breaks and phosphorylated H2AX, which is supposed to be associated with free ends of double-strand breaks.

SFGE was adopted to assess DNA double-strand breaks and their rejoining. With this approach, the amount of DNA breaks is estimated as the DNA released from a well into the gel after electrophoresis. The fraction of released DNA was shown to increase with radiation dose (*31*). As is indicated in Fig. 3A, immediately after exposure to 20 Gy, the amount of fragmented DNA released from the well showed an increase in all tissues of all genotypes compared to nonirradiated mice. However, 3.5 days after irradiation, the amount of fragmented DNA showed genotype- and tissue-specific differences. Fragmented DNA was much reduced in all three tissues of *Ku70*$^{+/-}$ mice. In *Ku70*$^{-/-}$ mice, on the other hand, a significant amount of DNA remained fragmented, showing suppression of DNA rejoining (Fig. 3). The statistical analysis comparing the amounts of fragmented DNAs in *Ku70*-deficient mouse tissues immediately and 3.5 days after 20 Gy irradiation showed that the rejoining was significant in liver ($P = 0.00877$) and brain ($P = 0.0104$) but not in spleen ($P = 0.0734$). This indicates that some DNA rejoining took place in the absence of *Ku70* but not as much as that observed in *Ku70*-proficient mice.

The presence of unrepaired DNA breaks in irradiated *Ku70*$^{-/-}$ mice was further indicated by the persistent presence of phosphorylated histone H2AX at 3.5 days postirradiation. Figure 4 shows Western blots of phosphorylated H2AX (γ-H2AX) in spleen, liver and brain at 1 h and 3.5 days after irradiation. In *Ku70*$^{+/-}$ mice, the γ-H2AX band observed at 1 h after irradiation disappeared at 3.5 days, whereas *Ku70*$^{-/-}$ mice showed significant levels of γ-H2AX at 3.5 days postirradiation, suggesting the persistent presence of unrepaired DNA breaks.

DISCUSSION

Double-strand breaks are considered to be the most important damage induced by ionizing radiation. Other types of lesions such as base damage and single-strand breaks, although more common, are repaired rapidly and do not have such disastrous consequences for cells if they are misrepaired, because they do not generally involve the loss of

TABLE 1
The Number of Deletion Mutations of Different Sizes Found in the Three Tissues

		Control			20 Gy		
Tissue	*Ku70*	Total mutations[a]	1–50 bp[b]	>50 bp[c]	Total mutations[a]	1–50 bp[b]	>50 bp[c]
Spleen	+/+, +/−	69	4 (5.8)[d]	0	64	34 (53.1)	4 (6.3)
	−/−	27	2 (7.4)	0	35	2 (5.7)	3 (8.6)
Liver	+/+, +/−	41	0	0	73	40 (54.8)	1 (1.4)
	−/−	25	3 (12.0)	0	37	5 (13.5)	3 (8.1)
Brain	+/+, +/−	47	7 (14.9)	0	51	15 (29.4)	1 (2.0)
	−/−	35	2 (5.7)	0	37	3 (8.1)	3 (8.1)

[a] Total number of independent mutations found.
[b] Number of deletion mutations of 1 to 50 bp.
[c] Number of deletion mutations of more than 50 bp.
[d] The numbers in parentheses indicate percentages.

DNA sequences from the genome. The present study demonstrates that NHEJ of DNA double-strand breaks is the major source of radiation-induced mutagenesis in mouse tissues. Double-strand breaks are only a minor component (about 1/250) of the total DNA damage (*34*). Since most of the radiation-induced mutations are suppressed in *Ku70*$^{-/-}$ mice (Fig. 1), it would appear that most DNA damage other than double-strand breaks is repaired correctly. It should be noted that a small number of mutations were induced in Ku70-deficient mice. These could be the result of mistakes in the other repair processes such as translesional DNA synthesis on damaged bases.

The number of DNA double-strand breaks induced by 1 Gy of radiation is estimated to be about 30 per cell with approximately 6×10^9 bp of total DNA (*34, 35*). The number of double-strand breaks induced in the 3.1-kbp-long *lacZ* gene by 20 Gy radiation would be estimated to be 30 $\times 10^{-5}$ ($30 \times 20 \times 3.1 \times 10^3/6 \times 10^9$). Since the number of radiation-induced mutations in the tissues is 23–32 $\times 10^{-5}$ (Fig. 1), the two numbers are similar. This suggests that each double-strand break in the *lacZ* gene leads to one mutation. This is reasonable because most radiation-induced double-strand breaks are accompanied by chemical alterations in one or more bases or the deoxyribose at the broken ends, and they must be removed before the break is sealed. In other words, the closeness of the estimated number of DNA double-strand breaks and the measured mutant frequency suggests that the fidelity of NHEJ is very poor for radiation-induced breaks.

One point that should be remembered in the interpreta-

TABLE 2
Multiple and Complex Type Mutations

Ku70	Dose (Gy)	Tissue	ID	Type[a]	Position[b]	Change[c]	Distance between the mutations (bp)
+/+	20	Spleen	M1-12	Multiple (−3, −1)	1456–1458, 1461	A T C C T T C C C G C → A T · · · T C C · G C	3
+/−	20	Liver	M1-16	Multiple (BS, BS)	2906	C A G T C → C A T T C	14
					2921	G A T G G → G A A G G	
		Brain	F2-10	Complex (−2, +1)	2351–2352	C C G C C G → C C T C G	—
−/−	0	Spleen	F2-7	Multiple (BS, BS, BS)	1111	G T C A G → G T T A G	11, 1
					1123, 1125	A T G A G C A → A T A A A C A	
	20	Spleen	M2-12	Multiple (BS, BS)	1187	T T C G C → T T T G C	993
					2181	C G T C T → C G C C T	
			M3-16	Multiple (BS, BS)	2392	A C G A C → A C A A C	558
					2951	C G C G G → C G T G G	
			M3-17	Multiple (BS, BS)	20	T T C A C → T T T A C	116
					1187	T T C G C → T T T G C	
		Liver	M2-16	Multiple (BS, BS)	452, 454	T G G C G T T → T G T C T T T	1
			F3-13	Complex (−1, +2)	881	T C G C T → T C A T C T	—
			F3-17	Multiple (BS, BS, +1)	1369, 1370, 1372	A C C C G A G T → A C A A G A A G T	2
		Brain	M3-4	Multiple (BS, BS)	154	A T C G C → A T T G C	1041
					1196	T C C G A → T C T G A	

[a] BS; base substitution, negative number; deletion, positive number; insertion.
[b] The position of nucleotide is numbered from the first nucleotide of initiation codon of the *lacZ* gene.
[c] The nucleotides showing alteration are underlined. The deleted nucleotides are shown by dots.

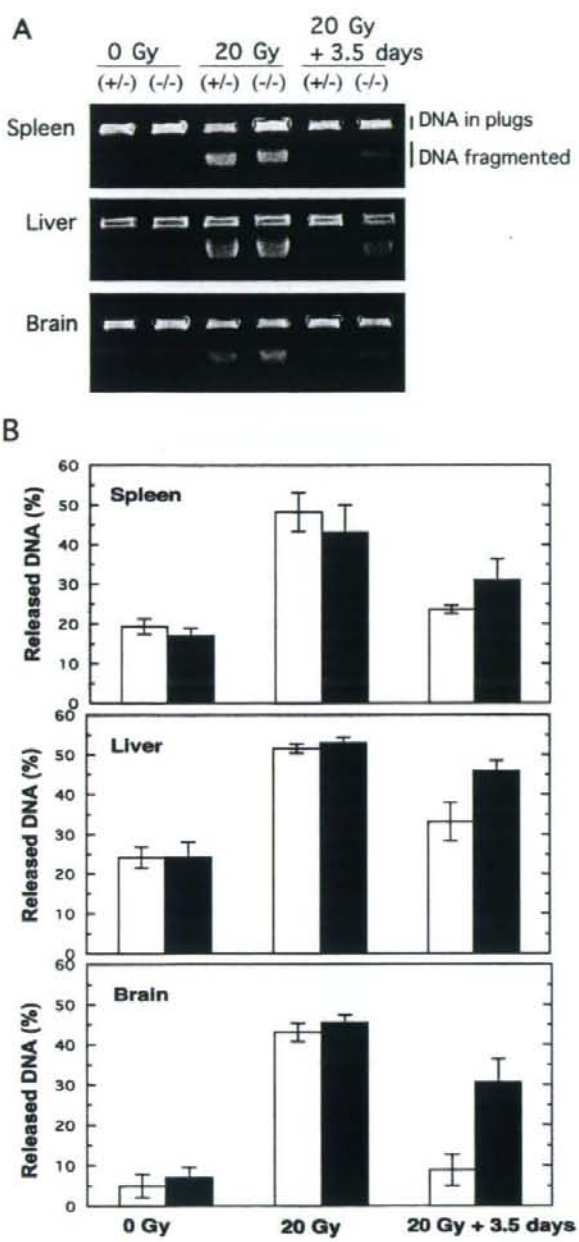

FIG. 3. SFGE analyses of DNA breaks and rejoining after 20 Gy of irradiation in *Ku70*-proficient $^{+/-}$ and deficient $^{-/-}$ mice. Panel A: Irradiation with 20 Gy increased the fraction of fragmented DNA which was released from the well in both *Ku70*$^{+/-}$ and $^{-/-}$ mice. At 3.5 days after irradiation, the fragmented DNA was reduced to the levels found in non-irradiated tissues in *Ku70*$^{+/-}$ mice and to intermediate levels in *Ku70*$^{-/-}$ mice. A similar trend was observed in the three tissues examined. Panel B: The experiment was repeated three times and the percentage of the fragmented DNA was quantified. The averages and standard deviations are shown. White columns represent *Ku70*$^{+/-}$ mice and the black columns *Ku70*$^{-/-}$ mice.

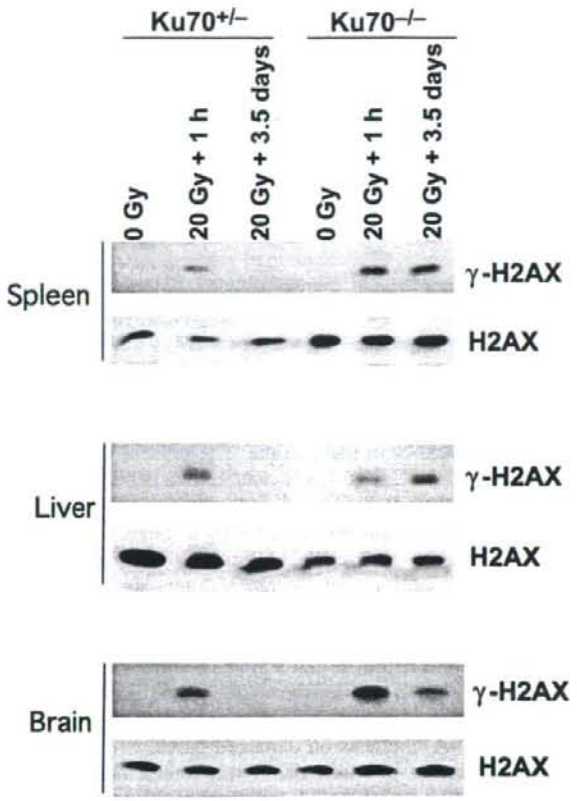

FIG. 4. Western blot analysis of the phosphorylation of histone H2AX. In *Ku70*-proficient mice, the phosphorylated H2AX (γ-H2AX) band was present at one hour after irradiation (20 Gy) and disappeared at 3.5 days in all tissues. In *Ku70*$^{-/-}$ mice, however, the γ-H2AX remained positive at 3.5 days after irradiation, suggesting that many of the radiation-induced DNA breaks remain unrepaired.

tion of the present results is that the mutational changes observed are limited to events within the 3.1-kbp-long *lacZ* gene. Therefore, large rearrangements such as deletions of more than a few kbp of DNA or translocation of the *lacZ* gene to the other chromosome cannot be detected in the present assay system, because each *lacZ* gene retrieved from the mouse genome needs to be packed into a λ phage to be analyzed for mutations. Thus the assay can monitor only base substitutions and deletions/insertions of up to a few kbp within or including the *lacZ* gene.

The other point to be noted is that the doses used in the present study are 20 Gy and 50 Gy. Although liver and brain tissue did not show any appreciable alterations after irradiation with those doses, the spleen was significantly smaller 3.5 days after irradiation. This is in accord with the prevalence of cell death in the spleen within 24 h after irradiation (*36*). Thus the data for spleen at 3.5 days after irradiation must represent the survival of only a minor fraction of spleen cells after these high doses. Further, defi-

ciency of Ku80, the other key protein of NHEJ, has been shown to enhance apoptosis in the spleen after irradiation (*36*). Thus it is possible that the reduction of radiation-induced mutations in the spleen of NHEJ-deficient mice reflects the preferential elimination of cells harboring a *lacZ* mutation. However, this is not likely, because it is difficult to imagine that the apoptosis induction system can work preferentially on cells that have damage or mutation on the *lacZ* gene. After irradiation with 20 Gy, each cell suffers significant DNA damage, including approximately 600 double-strand breaks, and no cell will be free of damage. The cells that have damage on the *lacZ* gene must have many other lesions on the other part of the genome. Under these conditions, it would be difficult to recognize selectively the cells containing damage in the *lacZ* gene. In addition, the *lacZ* gene used in the system does not have the promoter needed for transcription in mouse cells. Hence it is not expressed and could not be subject to selection by the cellular apoptosis system whether the gene is mutated or not.

Rothkamm *et al.* examined DNA ligation in cultured cells using pulsed-field gel electrophoresis and found that 50% of the double-strand breaks induced by an acute high dose of radiation (80 Gy) resulted in large DNA rearrangements, probably by ligation of illegitimate ends by NHEJ. The other 50% were ligated accurately without using the NHEJ repair system (*14*). Since the mutations monitored in the present study were small deletions of less than a few kbp within the *lacZ* gene, they must have belonged to the category considered to be "accurate ligation" in the study of Rothkamm *et al.* (*14*). At present, there is no way to estimate the ratio of mutation-free ligation and mutation-linked ligation in the "accurate ligation".

Our study as well as that of Rothkamm *et al.* (*14*) supports the existence of a functional double-strand break repair system other than NHEJ, because significant levels of DNA rejoining were observed after irradiation in NHEJ-deficient tissues and cells. It could be homologous recombination (HR) repair that functions as a form of error-free double-strand break repair when homologous DNA sequences are present. The strong repression of mutation induction in *Ku70*-deficient mouse tissues supports the importance of HR in these cells. It is also possible that microhomology-mediated end joining (MMEJ), which is error-prone and is suggested to be distinct from NHEJ (*3*), may function in NHEJ-deficient cells. Repair by MMEJ has been reported to result in relatively large deletions with short repeat sequences at the ends of deleted fragment (*3*). The frequency of repeated sequences at the ends of deleted DNA, a hallmark of MMEJ, was similar in both wild-type and *Ku70*-deficient mice (data not shown), which does not support a role for MMEJ. However, the deletion mutations observed in irradiated *Ku70*-deficient mice appear to contain slightly larger deletions than those in *Ku70*-proficient irradiated mice (Table 1), which may support the latter idea.

In the present study, we found nine multiple mutations (Table 2). Among them five cases showed two or three alterations located within a short stretch of nucleotides less than 30 bp long. This could be induced by clustered damage or by locally multiply damaged sites suggested by computer simulation of DNA damage (*37*). The other four multiple mutations displayed two base substitutions at separate positions located more than 500 bp apart. Since these were found only in irradiated *Ku70*-deficient mice, this type of mutation could be related to the NHEJ deficiency. Six out of eight base substitutions found in these multiple mutations were G:C to A:T transitions at CG sequences, a mutation type that is found most frequently in spontaneous mutations in vertebrates. Recently, Wang *et al.* proposed a phenomenon known as "mutation showers" as the cause of multiple mutations, which could occur as a result of a temporally unstable DNA polymerase or an imbalance in the deoxyribonucleotide triphosphate pool size (*38*). The multiple mutations observed in the present study could be explained by the same mechanism, although there is no evidence that Ku70 is involved in DNA polymerization or the maintenance of nucleotide pool levels.

In the present study we examined three tissues with different cell proliferation properties and asked whether there is any tissue specificity in mutation induction. The dose response of mutation induction revealed variation among the tissues, especially at 50 Gy (Fig. 1). The suppression of mutation induction at high doses could be explained by an increased probability of having two events in a single cell: mutation on the *lacZ* gene and a lethal hit for the cell. In fact, the strongest suppression was observed in the spleen, which was the most sensitive tissue among the three tissues examined. Brain cells would be more radioresistant than spleen and liver cells.

In conclusion, in *Ku70*$^{-/-}$ mice, end rejoining of X-ray-induced DNA breaks is impaired due to the absence of NHEJ repair, and the formation of mutations is suppressed. On the other hand, some non-NHEJ mediated DNA rejoining, which could be homologous recombination repair, appears to occur in *Ku70*-deficient animals.

ACKNOWLEDGMENTS

We thank Dr Frederick W. Alt for providing the *Ku70*$^{+/-}$ mice and Yasuko Syono, Yukiko Ikeda and Akemi Miura for technical support. The study was supported by grants from the "Ground-based Research Program for Space Utilization" promoted by the Japan Space Forum, the Budget for Nuclear Research of the Ministry of Education, Culture, Sports, Science and Technology, based on screening and counseling by the Atomic Energy Commission, and the NIFS Collaborative Research Program (NIFS07KOBS012).

Received: November 10, 2007; accepted: March 25, 2008

REFERENCES

1. M. R. Lieber, Y. Ma, U. Pannicke and K. Schwarz, Mechanism and regulation of human non-homologous DNA end-joining. *Nat. Rev. Mol. Cell Biol.* **4**, 712–720 (2003).

2. J. A. Downs and S. P. Jackson, A means to a DNA end: the many roles of Ku. *Nat. Rev. Mol. Cell Biol.* **5**, 367–378 (2004).
3. J. Thacker and M. Z. Zdzienicka, The XRCC genes: expanding roles in DNA double-strand break repair. *DNA Repair* **3**, 1081–1090 (2004).
4. S. Burma, B. P. C. Chen and D. J. Chen, Role of non-homologous end joining (NHEJ) in maintaining genomic integrity. *DNA Repair* **5**, 1042–1048 (2006).
5. D. Buck, L. Malivert, R. de Chasseval, A. Barraud, M-C. Fondanèche, O. Sanal, A. Plebani, J-L. Stéphan, M. Hufnagel and P. Revy, Cernunnos, a novel nonhomologous end-joining factor, is mutated in human immunodeficiency with microcephaly. *Cell* **124**, 287–299 (2006).
6. P. Ahnesorg, P. Smith and S. P. Jackson, XLF interacts with the XRCC4-DNA ligase IV complex to promote DNA nonhomologous end-joining. *Cell* **124**, 301–313 (2006).
7. A. Nijnik, L. Woodbine, C. Marchetti, S. Dawson, T. Lambe, C. Liu, N. P. Rodrigues, T. L. Crockford, E. Cabuy and R. J. Cornall, DNA repair is limiting for haematopoietic stem cells during ageing. *Nature* **447**, 686–693 (2007).
8. D. J. Rossi, D. Bryder, J. Seita, A. Nussenzweig, J. Hoeijmakers and I. L. Weissman, Deficiencies in DNA damage repair limit the function of haematopoietic stem cells with age. *Nature* **447**, 725–729 (2007).
9. Z. E. Karanjawala, U. Grawunder, C-L. Hsieh and M. R. Lieber, The nonhomologous DNA end joining pathway is important for chromosome stability in primary fibroblasts. *Curr. Biol.* **9**, 1501–1506 (1999).
10. D. O. Ferguson, J. M. Sekiguchi, S. Chang, K. M. Frank, Y. Gao, R. A. DePinho and F. W. Alt, The nonhomologous end-joining pathway of DNA repair is required for genomic stability and the suppression of translocations. *Proc. Natl. Acad. Sci. USA* **97**, 6630–6633 (2000).
11. M. J. Difillppantonlo, J. Zhu, H. T. Chen, E. Meffre, M. C. Nussenwig, E. E. Max, T. Ried and A. Nussenzweig, DNA repair protein Ku80 suppresses chromosomal aberrations and malignant transformation. *Nature* **404**, 510–514 (2000).
12. L. D. Rockwood, A. Nussenzweig and S. Janz, Paradoxical decrease in mutant frequencies and chromosomal rearrangements in a transgenic *lacZ* reporter gene in Ku80 null mice deficient in DNA double strand break repair. *Mutat. Res.* **529**, 51–58 (2003).
13. M. Martín, A. Genescà, L. Latre, I. Jaco, G. E. Taccioli, J. Egozcue, M. A. Blasco, G. Iliakis and L. Tusell, Postreplicative joining of DNA double-strand breaks causes genomic instability in DNA-PKcs-deficient mouse. *Cancer Res.* **65**, 10223–10232 (2005).
14. K. Rothkamm, M. Kühne, P. A. Jeggo and M. Löbrich, Radiation-induced genomic rearrangements formed by nonhomologous end-joining of DNA double-strand breaks. *Cancer Res.* **61**, 3886–3893 (2001).
15. Y. Peng, Q. Zhang, H. Nagasawa, R. Okayasu, H. L. Liber and J. S. Bedford, Silencing expression of the catalytic subunit of DNA-dependent protein kinase by small interfering RNA sensitizes human cells for radiation-induced chromosome damage, cell killing, and mutation. *Cancer Res.* **62**, 6400–6404 (2002).
16. T. Zhou and L. F. Povirk, Extreme cytotoxicity and susceptibility to hprt mutagenesis in Ku-deficient xrs-6 cells treated with bleomycin in plateau phase. *Mutagenesis* **20**, 39–44 (2005).
17. T. Ono, H. Ikehata, S. Nakamura, Y. Saito, J. Komura, Y. Hosoi and K. Yamamoto, Molecular nature of mutations induced by a high dose of X-rays in spleen, liver, and brain of the *lacZ*-transgenic mouse. *Environ. Mol. Mutagen.* **34**, 97–105 (1999).
18. K. Masumura, K. Kuniya, T. Kurobe, M. Fukuoka, F. Yatagai and T. Nohmi, Heavy-ion-induced mutations in the gpt delta transgenic mouse: comparison of mutation spectra induced by heavy-ion, X-ray, and γ-ray radiation. *Environ. Mol. Mutagen.* **40**, 207–215 (2002).
19. Y. Gu, S. Jin, Y. Gao, D. T. Weaver and F. W. Alt, Ku70-deficient embryonic stem cells have increased ionizing radiosensitivity, defective DNA end-binding activity, and inability to support V(D)J recombination. *Proc. Natl. Acad. Sci. USA* **94**, 8076–8081 (1997).
20. F. Liang, M. Han, P. J. Romanienko and M. Jasin, Homology-directed repair is a major double-strand break repair pathway in mammalian cells. *Proc. Natl. Acad. Sci. USA* **95**, 5172–5177 (1998).
21. M. Honma, M. Izumi, M. Sakuraba, S. Tadokoro, H. Sakamoto, W. Wang, F. Yatagai and M. Hayashi, Deletion, rearrangement, and gene conversion: genetic consequences of chromosomal double-strand breaks in human cells. *Environ. Mol. Mutagen.* **42**, 288–298 (2003).
22. M. Honma, M. Sakuraba, T. Koizumi, Y. Takashima, H. Sakamoto and M. Hayashi, Non-homologous end-joining for repairing I-SceI-induced DNA double strand breaks in human cells. *DNA Repair* **6**, 781–788 (2007).
23. M. E. T. Dollé, W. K. Snyder, J. A. Gossen, P. H. M. Lohman and J. Vijg, Distinct spectra of somatic mutations accumulated with age in mouse heart and small intestine. *Proc. Natl. Acad. Sci. USA* **97**, 8403–8408 (2000).
24. T. Ono, H. Ikehata, V. P. Pithani, Y. Uehara, Y. Chen, Y. Kinouchi, T. Shimosegawa and Y. Hosoi, Spontaneous mutations in digestive tract of old mice show tissue-specific patterns of genomic instability. *Cancer Res.* **64**, 6919–6923 (2004).
25. T. Ono, H. Ikehata, Y. Uehara and J. Komura, The maintenance of genome integrity is tissue-specific. *Genes Environ.* **28**, 16–22 (2006).
26. K. E. Orii, Y. Lee, N. Kondo and P. J. McKinnon, Selective utilization of nonhomologous end-joining and homologous recombination DNA repair pathways during nervous system development. *Proc. Natl. Acad. Sci. USA* **103**, 10017–10022 (2006).
27. L. Brugmans, R. Kanaar and J. Essers, Analysis of DNA double-strand break repair pathways in mice. *Mutat. Res.* **614**, 95–108 (2007).
28. J. A. Gossen, W. J. F. de Leeuw, C. H. T. Tan, E. C. Zwarthoff, F. Berends, P. H. M. Lohman, D. L. Knook and J. Vijg, Efficient rescue of integrated shuttle vectors from transgenic mice: a model for studying mutations *in vivo*. *Proc. Natl. Acad. Sci. USA* **86**, 7971–7975 (1989).
29. Y. Gu, K. J. Seidl, G. A. Rathbun, C. Zhu, J. P. Manis, N. van der Stoep, L. Davidson, H-L. Cheng and F. W. Alt, Growth retardation and leaky SCID phenotype of Ku70-deficient mice. *Immunity* **7**, 653–665 (1997).
30. F. Wang, Y. Saito, T. Shiomi, S. Yamada, T. Ono and H. Ikehata, Mutation spectrum in UVB-exposed skin epidermis of a mildly-affected Xpg-deficient mouse. *Environ. Mol. Mutagen.* **47**, 107–116 (2006).
31. R. Hirayama, Y. Furusawa, T. Fukawa and K. Ando, Repair kinetics of DNA-DSB induced by X-rays or carbon ions under oxic and hypoxic conditions. *J. Radiat. Res.* **46**, 325–332 (2005).
32. J. Sambrook and D. W. Russell, SDS-polyacrylamide gel electrophoresis of proteins. *In Molecular Cloning- A Laboratory Manual*, 3rd ed. (J. Sambrook and D. W. Russell, Eds.), pp. A8.40–A8.55. Cold Spring Harbor Laboratory Press, Cold Spring Harbor, NY, 2001.
33. K. Rothkamm and M. Löbrich, Evidence for a lack of DNA double-strand break repair in human cells exposed to very low x-ray doses. *Proc. Natl. Acad. Sci. USA* **100**, 5057–5062 (2003).
34. J. F. Ward, DNA damage produced by ionizing radiation in mammalian cells: identities, mechanisms of formation, and reparability. *Prog. Nucleic Acids Res. Mol. Biol.* **35**, 95–125 (1988).
35. B. Stenerlöw, K. H. Karlsson, B. Cooper and B. Rydberg, Measurement of prompt DNA double-strand breaks in mammalian cells without including heat-labile sites: Results for cells deficient in nonhomologous end joining. *Radiat. Res.* **159**, 502–510 (2003).
36. A. Nussenzweig, K. Sokol, P. Burgman, L. Li and G. C. Li, Hypersensitivity of *Ku80*-deficient cell lines and mice to DNA damage: The effects of ionizing radiation on growth, survival, and development. *Proc. Natl. Acad. Sci. USA* **94**, 13588–13593 (1997).
37. H. Nikjoo, P. O'Neill, D. T. Goodhead and M. Terrissol, Computational modelling of low-energy electron-induced DNA damage by early physical and chemical events. *Int. J. Radiat. Biol.* **71**, 467–483 (1997).
38. J. Wang, K. D. Gonzalez, W. A. Scaringe, K. Tsai, N. Liu, D. Gu, W. Li, K. A. Hill and S. S. Sommer, Evidence for mutation showers. *Proc. Natl. Acad. Sci. USA* **104**, 8403–8408 (2007).

H., Poeck, H., Akira, S., Conzelmann, K.K., Schlee, M., Endres, S., & Hartmann, G. (2006) *Science*, 314, 994–997.
8) Pichlmair, A., Schulz, O., Tan, C.P., Naslund, T.I., Liljestrom, P., Weber, F., & Reis e Sousa, C. (2006) *Science*, 314, 997–1001.
9) Kato, H., Takeuchi, O., Mikano-Satoh, E., Hirai, R., Kawai, T., Matsushita, K., Hiiragi, A., Dermody, T.S., Fujita, T., & Akira, S. (2008) *J. Exp. Med.*, 205, 1601–1610.
10) Takahasi, K., Yoneyama, M., Nishihori, T., Hirai, R., Kumeta, H., Narita, R., Gale, M., Jr., Inagaki, F., & Fujita, T. (2008) *Mol. Cell*, 29, 428–440.
11) Cui, S., Eisenacher, K., Kirchhofer, A., Brzozka, K., Lammens, A., Lammens, K., Fujita, T., Conzelmann, K.K., Krug, A., & Hopfner, K.P. (2008) *Mol. Cell*, 29, 169–179.

米山 光俊[1,2]，藤田 尚志[1]
([1]京都大学ウイルス研究所・分子遺伝学研究分野，
[2]科学技術振興機構さきがけ研究員)

Non-self RNA-sensing mechanism of RIG-I RNA helicase
Mitsutoshi Yoneyama[1,2] and Takashi Fujita[1] ([1]Laboratory of Molecular Genetics, Institute for Virus Research, Kyoto University, 53 Shogoinkawahara-cho, Sakyo-ku, Kyoto 606–8507, Japan; [2]PRESTO, Japan Science and Technology Agency, 4–1–8 Honcho Kawaguchi, Saitama 332–0012, Japan)

誘発突然変異と損傷乗り越えDNA合成 —REV1の構造と生化学的機能—

1. はじめに

誘発突然変異は，電離放射線や紫外線，化学物質などの変異誘発剤によって誘発される突然変異を指す．変異誘発剤はWatson-Crick型の塩基対合を変化させるようなDNA損傷を引き起こすが，突然変異が誘発されるためには，DNA損傷に加えて細胞内の積極的な機能が必要不可欠である．*REV1*遺伝子（reversionless）は，この突然変異誘発に必要不可欠な酵母の遺伝子として同定された．本稿では，酵母及びヒトREV1の構造と生化学的特性から突然変異誘発における機能を概説する．

2. 誘発突然変異と損傷乗り越えDNA合成

細胞に紫外線が照射されると，新生DNA鎖の断片化が観察される．これは，複製型のDNAポリメラーゼ（pol δまたはpol ε）が，紫外線損傷に対してDNA伸長反応を停止することに起因する．その後，この断片化したDNAはより大きなDNAに移行するが，この過程を複製後修復（post-replication repair）と呼ぶ．複製後修復では，損傷塩基は除去せずに，断片化したDNAどうしを繋げることにより，複製過程で生じたギャップを修復する[1,2]．

酵母では，*RAD*（radiation sensitivity）遺伝子群として同定された遺伝子の中で，複製後修復に関与する遺伝子群は*RAD6*エピスタシス群として分類される．複製後修復経路は，ユビキチンリガーゼE2-E3であるRAD6-RAD18複合体によるproliferating cell nuclear antigen（PCNA）のモノユビキチン化により制御される．損傷乗り越えDNA合成（translesion DNA synthesis, TLS）経路はRAD6-RAD18の下流で機能する複製後修復経路の一つである．TLS経路では，特殊なDNAポリメラーゼ（TLSポリメラーゼ）が，損傷塩基を鋳型としたDNA合成反応により，DNA複製を回復する[1,2]．

酵母の*REV1*遺伝子は，紫外線による突然変異の誘発が抑制される変異体として同定された．*rev1*株では，紫外線や電離放射線をはじめ，様々な種類の薬剤による突然変異の誘発が抑制され，同時にそれら薬剤に対する感受性が増大する[3]．Lawrenceのグループは1996年に酵母のREV1タンパク質がDNA損傷の一つ，脱塩基部位（DNA上の塩基が脱離しデオキシリボースだけになった状態のDNA損傷）に対して，dCMPを対合するデオキシシチジルトランスフェラーゼであることを発見した[4]．

一方，色素性乾皮症バリアント群（XP-V）に分類される患者由来の細胞では，紫外線による誘発突然変異頻度が高いこと，紫外線照射後の複製後修復に欠損のあることが知られていた[2]．花岡のグループは1999年にXP-Vの責任遺伝子がシクロブタン型チミンダイマーに対してdAMPを対合する活性をもつpol ηをコードすることを明らかにした[5]．TLS経路で機能するこれらの酵素は構造的に類似しており，Y-ファミリーのDNAポリメラーゼとして分類されている[6]．XP-Vの患者由来の細胞ではpol ηの代わりに，別のTLSポリメラーゼが働き，dAMP以外の塩基を挿入した結果，突然変異頻度が上昇すると考えられている[2]．

Y-ファミリーのDNAポリメラーゼは，原核生物から高等真核生物まで広く保存されており，ヒトではpol η，pol ι，pol κ，REV1の4種類が存在する（図1）[6]．REV1はY-ファミリーのメンバーではあるが，その活性はdCMP転移活性に限られ，他の基質dATP，dGTP，dTTPに対する親和性は極めて低く，実質上ポリメラーゼ活性はない．真核生物のポリメラーゼでは，触媒ドメイン以外にも多くの類似

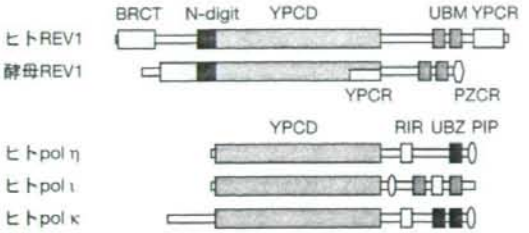

図1 Y-ファミリーDNAポリメラーゼの構造

BRCT: BRCA1 C-terminus domain, YPCD: Y-family DNA polymerase catalytic domain, YPCR: Y-family DNA polymerase contacting region, PZCR: polymerase ζ contacting region, UBM: ubiquitin binding motif, UBZ: ubiquitin binding Zn finger, PIP: PCNA interacting protein box, RIR: REV1 interacting region.

点がある（図1）[6]．ユビキチン結合ドメイン（UBMまたはUBZ），PCNAと結合する配列（PIP box）は，Y-ファミリーのポリメラーゼが損傷部位で機能する際，ユビキチン化されたPCNAと相互作用するために必要であると考えられている．また，全てのポリメラーゼにはREV1と相互作用する領域が同定されているが，この相互作用の意義は今のところ不明である．

3. TLS酵素としてのREV1の構造と機能

REV1のdCMP転移活性は，鋳型Gに対する効率が最も高いが，損傷部位としては脱塩基部位に対して効率よくdCMPを対合する[4,7]．REV1がdCTPを認識する分子機構はとてもユニークである．REV1は触媒ドメインのN末端側にREV1に特徴的なドメイン（N-digit）をもち，この中のアルギニン残基がシトシンとの水素結合によりdCTPを認識する．一方，鋳型Gは外側に追い出され，空いた間隙はアルギニン残基に隣接するロイシン酸残基により占められる[8]．脱塩基部位に対する結合もこのロイシン残基により安定化されるものと思われる．生体内では，DNA上のあらゆる塩基が脱離することによって脱塩基部位が生じると考えられ，脱塩基部位に対するdCMPの取り込みは，塩基置換の原因となりうる[9]．REV1はdCTPの選択性に関してとても巧妙な構造をもつが，なぜ取り込まれる塩基がdCMPであるのか，その生物学的理由は明らかでない．

REV1のdCMP転移活性が，細胞内でTLSに機能しているという証拠は，酵母を使った研究から示されている．Dempleのグループは，チミンまたはシトシン塩基をDNAから除去する活性を獲得した変異型DNAグリコシラーゼを酵母で発現させ，生じた脱塩基部位に挿入される塩基を解析した[6]．その結果，どちらのグリコシラーゼを発現させた場合にも突然変異頻度が上昇し，その大部分にREV1依存的なdCMPの挿入が観察された．

4. REV1の第二の機能と構造

酵母では*REV1*遺伝子が欠損すると様々なDNA損傷に対して感受性となると同時に，突然変異の誘発が抑制される．実際に，T-T（6-4）光産物を含むプラスミドを酵母に導入しそのTLSを解析すると，約7割のケースでdAMPの取り込みによる正しいTLSが観察され，3割のケースでdTMPまたはdGMPの挿入による誤ったTLSが観察される．興味深いことに，どちらのTLSも*REV1*依存的であるにもかかわらず，dCMPの挿入が観察されない．さらに，このTLSにはREV1の触媒活性は必要なく，むしろBRCTドメインが必要であることから，REV1の第二の機能と呼ばれている[2]．REV1が関与する多くのTLSと突然変異誘発は，この第二の機能が関わっている．

酵母の遺伝学的解析では，*REV1*は他の*REV*遺伝子，*REV3*，*REV7*とエピスタティックである．したがって，突然変異誘発におけるREV1の機能（REV1の第二の機能）はREV3，REV7と同一の生化学的過程にあると予想される[3]．*REV3*はpol ζの触媒サブユニット，*REV7*は非触媒サブユニットをコードし，安定な複合体pol ζを構成する．pol ζはY-ファミリーのTLSポリメラーゼとは構造的に異なったもう一つのTLSポリメラーゼである[3]．酵母のREV1では，pol ζと相互作用する部位が同定され（図1），REV1によるpol ζの活性促進が観察される．また，その領域を欠失したREV1では紫外線感受性を示すと同時に，突然変異の誘発が見られないことから，REV1の第二の機能のある部分は，この相互作用を介したpol ζの活性促進によるものであると考えられる[3]．しかしヒトにおいては，REV1とpol ζとの相互作用は明らかになっていない．

REV1に特徴的なもう一つの構造として，他のY-ファミリーのポリメラーゼと相互作用する領域が同定されている（図1）[8]．この領域は，REV7と結合することによりREV1-REV7複合体の構成にも必要とされる[10,11]．不思議なことにREV7はREV1のdCMP転移活性に全く影響を与えない[11]．また，REV7の結合はREV1と他のY-ファミリーポリメラーゼとの相互作用を阻害する[5]．これらの結果は，TLSにおけるポリメラーゼの選択等の調節にREV7が関与することを示唆するのかもしれない．

REV1は他のポリメラーゼとは異なり，PCNAと相互作用するPIP boxが見いだされない．実際に，酵母REV1はPCNAにより活性化されないという報告があり[12]，我々も

ヒトREV1で同様の結果を得ている．一方で，PCNAが酵母REV1のC末端側と相互作用し，活性化するという報告もある[13]．この活性化は，ユビキチン化されたPCNAによりさらに促進され，REV1のUBMに依存する．この結果は酵母の遺伝学によっても支持され，UBMを欠失した*rev1*では紫外線感受性を示すと同時に突然変異が誘発されない．一方これらの結果に反して，マウスRev1ではBRCTドメインがPCNAと相互作用するとの報告もあり[14]，これらの矛盾が解決されるためにはさらなる解析が必要である．

5. REV1の単鎖DNA結合活性

我々は，REV1が単鎖DNA結合活性をもつことを見いだした[15]．この活性がREV1のdCMP転移反応にどのように作用するかを調べるために，長さの違う3種類のプライマーテンプレートを作成した（図2Aa–c下段）．これらのプライマーテンプレートとREV1を反応させると全て同等にdCMPが重合された（図2Aa–c）．また，短い鋳型からなる二つのプライマーテンプレートを同時に反応させるとREV1は両方のプライマー末端に同様にdCMPを重合した（図2Ad）．ところが長い鋳型と短い鋳型からなるプライマーテンプレートを同時に反応させると，長い鋳型からなるプライマーに選択的に反応が観察された（図2Ae）これらの結果は，単鎖DNAに結合したREV1はその単鎖DNA上にあるプライマー末端に選択的にターゲティングされることを示しており，この過程でREV1は単鎖DNA上をスライディングしていると思われる．この性質は欠失型REV1（M5）で消失し（図2BC），polηでは観察されないことから[15]，REV1特異的である．これらの結果は，REV1の最初のターゲットが単鎖DNAである可能性を示唆する[15]．

おわりに

REV1の構造とその生化学的特性は酵母からヒトまでとてもよく保存されていることが明らかとなった．REV1は様々なタンパク質と相互作用し，Y-ファミリーのメンバーの中では，構造的，機能的に特殊な存在である．これらの相互作用は，TLSを制御するためのものであると考えられる．しかし，これまでに報告されている実験結果は依然断片的であり，REV1と突然変異誘発機構の全体像解明にはさらなる研究が必要である．

1) Andersen, P.L., Xu, F., & Xiao, W. (2008) *Cell Res.*, 18, 162–173.
2) Lehmann, A.R., Niimi, A., Ogi, T., Brown, S., Sabbioneda, S., Wing, J.F., Kannouche, P.L., & Green, C.M. (2007) *DNA Repair (Amst.)*, 6, 891–899.
3) Lawrence, C.W. (2002) *DNA Repair (Amst.)*, 1, 425–435.
4) Nelson, J.R., Lawrence, C.W., & Hinkle, D.C. (1996) *Nature*, 382, 729–731.
5) Masutani, C., Kusumoto, R., Yamada, A., Dohmae, N., Yokoi, M., Yuasa, M., Araki, M., Iwai, S., Takio, K., & Hanaoka, F.

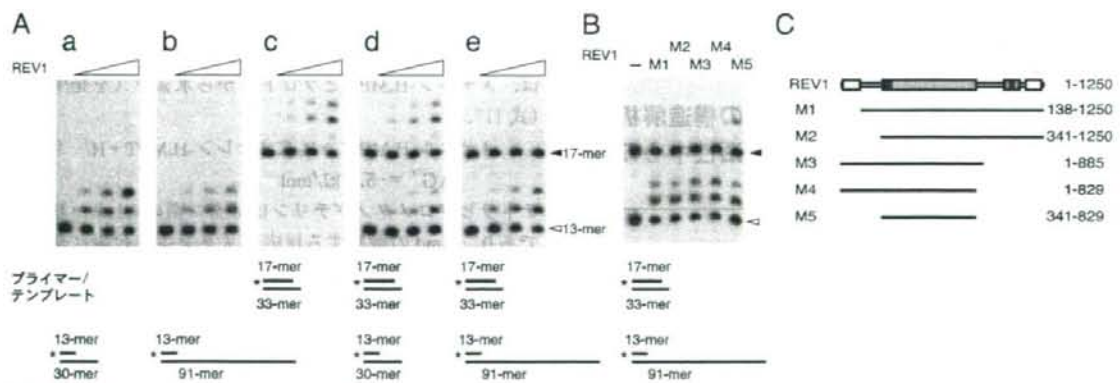

図2 単鎖DNAを介したREV1のターゲティング

A．REV1のdCMP転移反応における選択的反応性．^{32}Pで標識した（*）様々な長さのプライマーテンプレート（下段に記載）とREV1を反応させた．

B．欠失型REV1のdCMP転移反応における選択的反応性．下段に示したプライマーテンプレートと欠失型REV1を反応させた．反応産物は変性アクリルアミドゲル電気泳動後，オートラジオグラムにより解析した．

C．欠失型REV1の構造．